

# Multi-Scale Investigations of Flux transfer events (FTEs) and Kelvin-Helmholtz waves/vortices (KHWs/KHVs)

Kyoung-Joo ('Joo') Hwang (1)

Eunjin Choi (1), Kyunghwan Dokgo (1), J. L. Burch (1), D. G. Sibeck (2), B. L. Giles (2), C. J. Pollock (3), R. Fear (4), T.K.M. Nakamura (5), H. Fu (6), C. P. Escoubet (7), S. Toledo-Redondo (8), B. Lauvrad (8), Y. Khotyaintsev (9), D. Graham (9), C. Norgren (10), X. Ma (11), D. Gershman (2), R. E. Ergun (12), R. B. Torbert (13), J. C. Dorelli (2), L. Avanov (2), W. R. Paterson (2), C. T. Russell (14), and R. J. Strangeway (14) + **ISSI MMS-Cluster RX team**

(1) Southwest Research Institute, San Antonio, TX

(2) NASA Goddard Space Flight Center, Greenbelt, MD

(3) Denali Scientific, LLC, Alaska, AK

(4) University of Southampton, UK

(5) Austrian Academy of Sciences, Space Research Institute, Vienna, Austria

(6) School of Science and Environment, Beihang University, China

(7) European Space Research and Technology Centre, Noordwijk, Netherlands

(8) Institut de Recherche en Astrophysique et Planétologie, CNRS, UPS, CNES, Université de Toulouse, Toulouse, France

(9) Swedish Institute of Space Physics, Uppsala, Sweden

(10) University of Bergen, Bergen, Norway

(11) Physical Sciences Department, Embry-Riddle Aeronautical University, Daytona Beach, FL

(2) Laboratory for Atmospheric and Space Physics, University of Colorado at Boulder, Boulder, CO

(13) Space Science Center, University of New Hampshire, Durham, NH

(14) Institute of Geophysics and Planetary Physics, University of California, Los Angeles, Los Angeles, CA

**Acknowledgements: MMS FPI, Fields, EPD, and Theory/Modeling teams**

# Multi-Scale Investigations of Flux transfer events (FTEs) and

**Kelvin-Helmholtz waves/vortices (KHWs/KHVs)**

**Kyoung-Joo ('Joo') Hwang (1)**

**Eunjin Choi (1), Kyunghwan Dokgo (1), J. L. Burch (1), D. G. Sibeck (2), B. L. Giles (2), C. J. Pollock (3), R. Fear (4), T.K.M. Nakamura (5), H. Fu (6), C. P. Escoubet (7), S. Toledo-Redondo (8), B. Lavrad (8), Y. Khotyaintsev (9), D. Graham (9), C. Norgren (10), X. Ma (11), D. Gershman (2), R. E. Ergun (12), R. B. Torbert (13), J. C. Dorelli (2), L. Avanov (2), W. R. Paterson (2), C. T. Russell (14), and R. J. Strangeway (14) + ISSI MMS-Cluster RX team**

(1) Southwest Research Institute, San Antonio, TX

(2) NASA Goddard Space Flight Center, Greenbelt, MD

(3) Denali Scientific, LLC, Alaska, AK

(4) University of Southampton, UK

(5) Austrian Academy of Sciences, Space Research Institute, Vienna, Austria

(6) School of Science and Environment, Beihang University, China

(7) European Space Research and Technology Centre, Noordwijk, Netherlands

(8) Institut de Recherche en Astrophysique et Planétologie, CNRS, UPS, CNES, Université de Toulouse, Toulouse, France

(9) Swedish Institute of Space Physics, Uppsala, Sweden

(10) University of Bergen, Bergen, Norway

(11) Physical Sciences Department, Embry-Riddle Aeronautical University, Daytona Beach, FL

(2) Laboratory for Atmospheric and Space Physics, University of Colorado at Boulder, Boulder, CO

(13) Space Science Center, University of New Hampshire, Durham, NH

(14) Institute of Geophysics and Planetary Physics, University of California, Los Angeles, Los Angeles, CA

**Acknowledgements: MMS FPI, Fields, EPD, and Theory/Modeling teams**

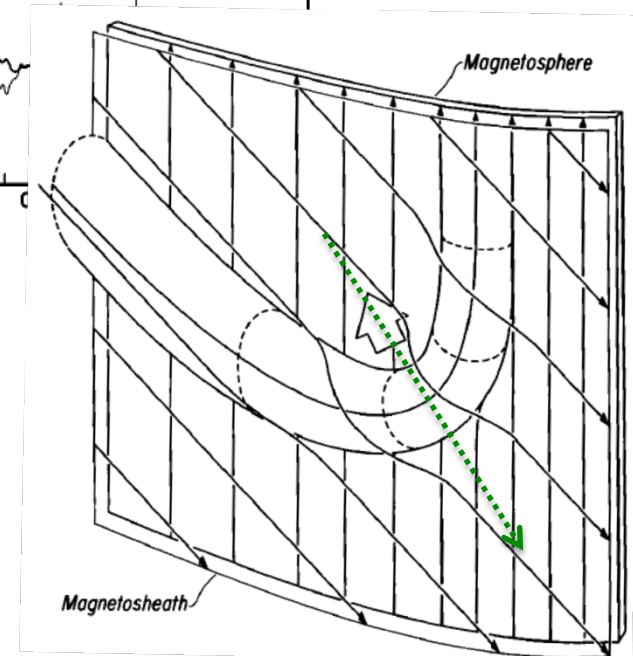
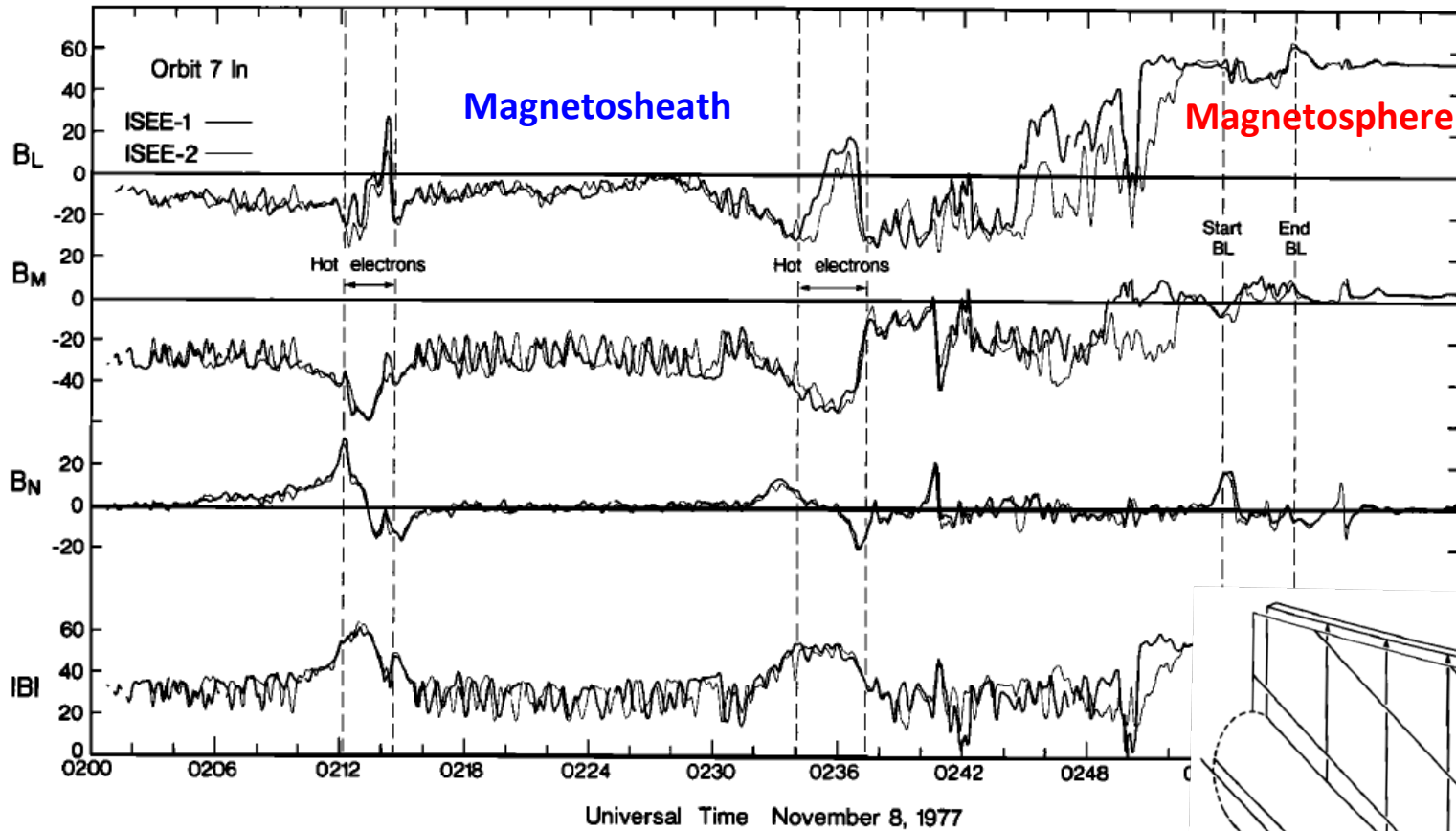
# Outline

1. **FTE: general knowns**
2. **Reconnection-based FTE models**
3. **New findings on FTE after MMS**
4. **Velocity-shear-induced FTE**

# Outline

1. **FTE: general knowns**
2. **Reconnection-based FTE models**
3. **New findings of FTE after MMS**
4. **Velocity-shear-induced FTE**

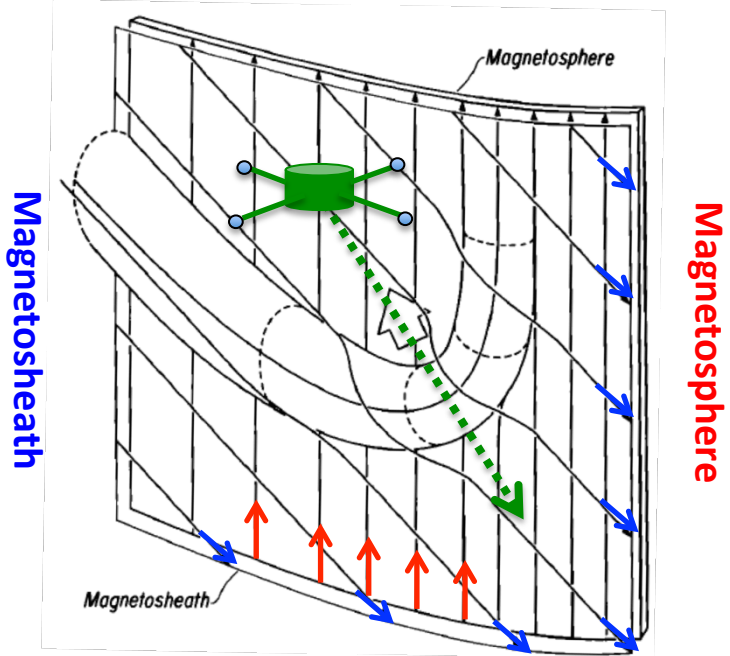
# FTE: Initial In-situ Observation



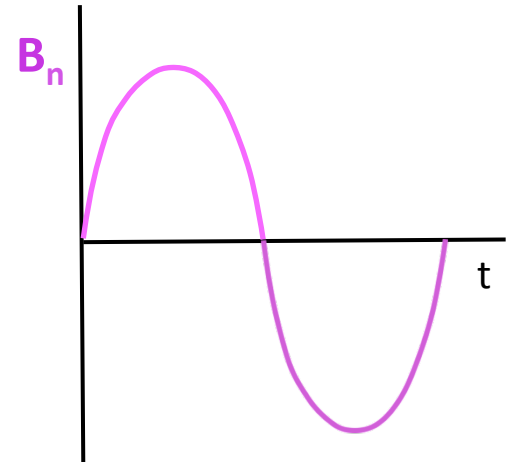
## Russell & Elphic [1978; 1979]

- Introduced boundary normal coordinate system (LMN)
- Identified **bipolar  $B_n$**  signature &  **$|B|$  enhancement**
- Interpreted as signature of localized flux ropes, 'flux transfer events'

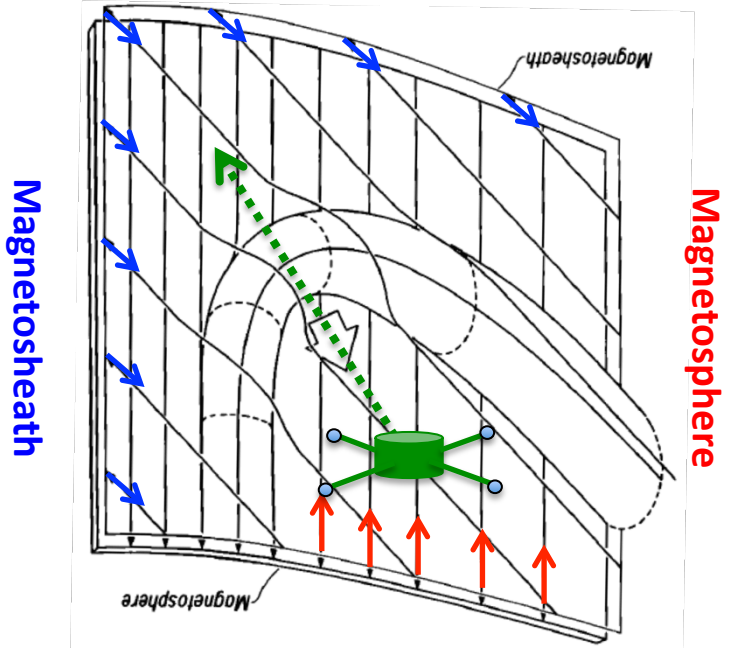
# FTE: $B_n$ polarity representing a motion - 1



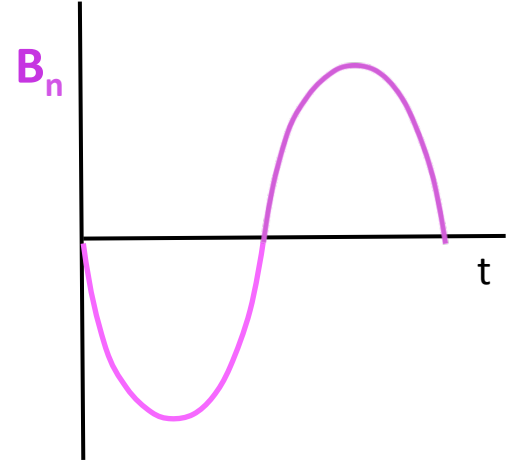
Northward motion (standard polarity):



Russell & Elphic [1978]

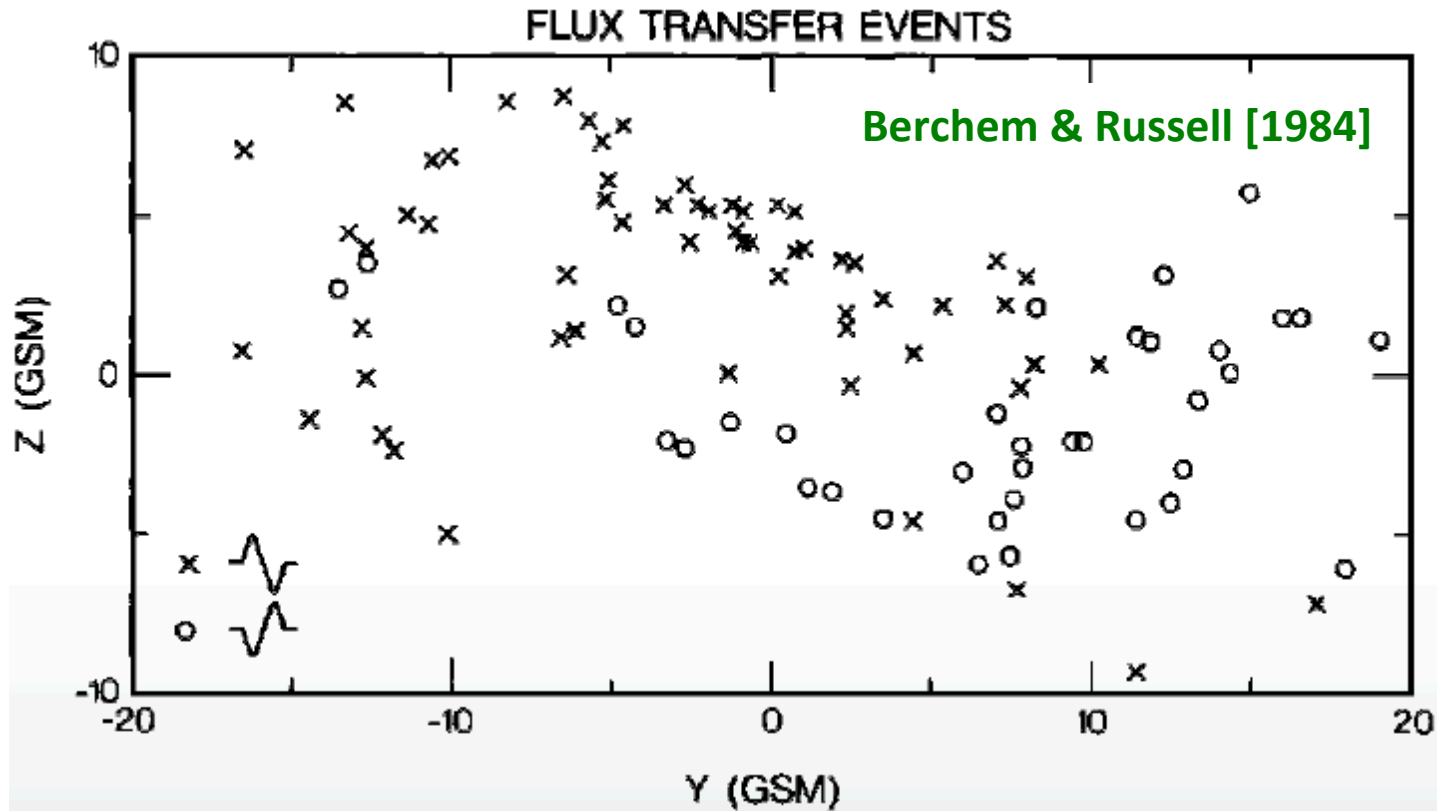


Southward motion (reverse polarity):



Rijnbeek et al. [1982]

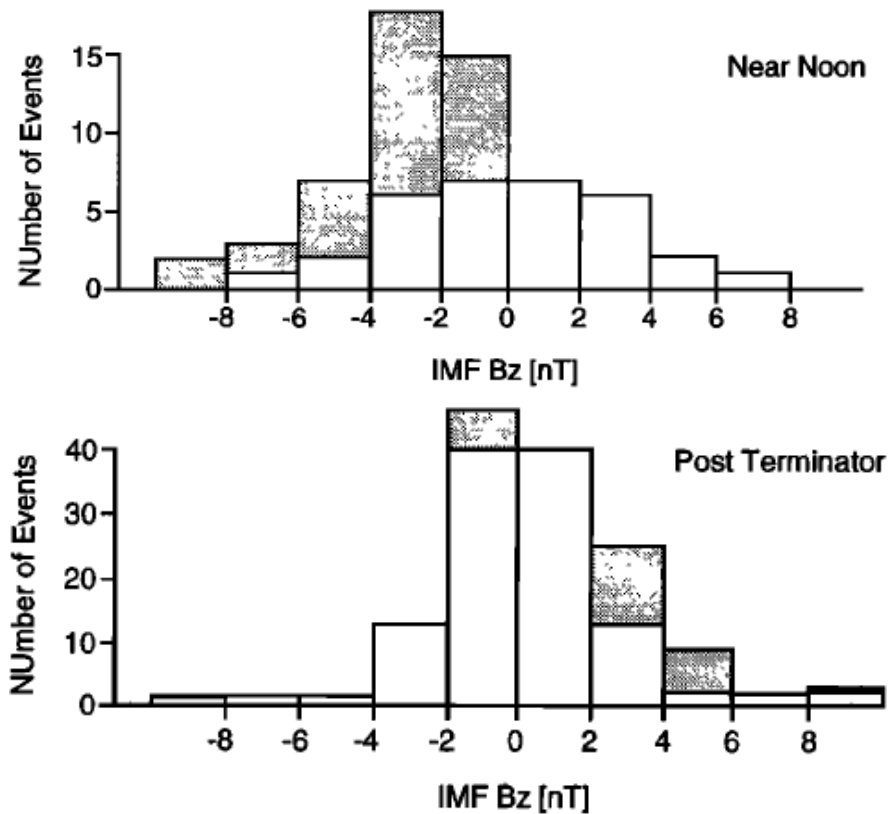
# FTE: $B_n$ polarity representing a motion - 2



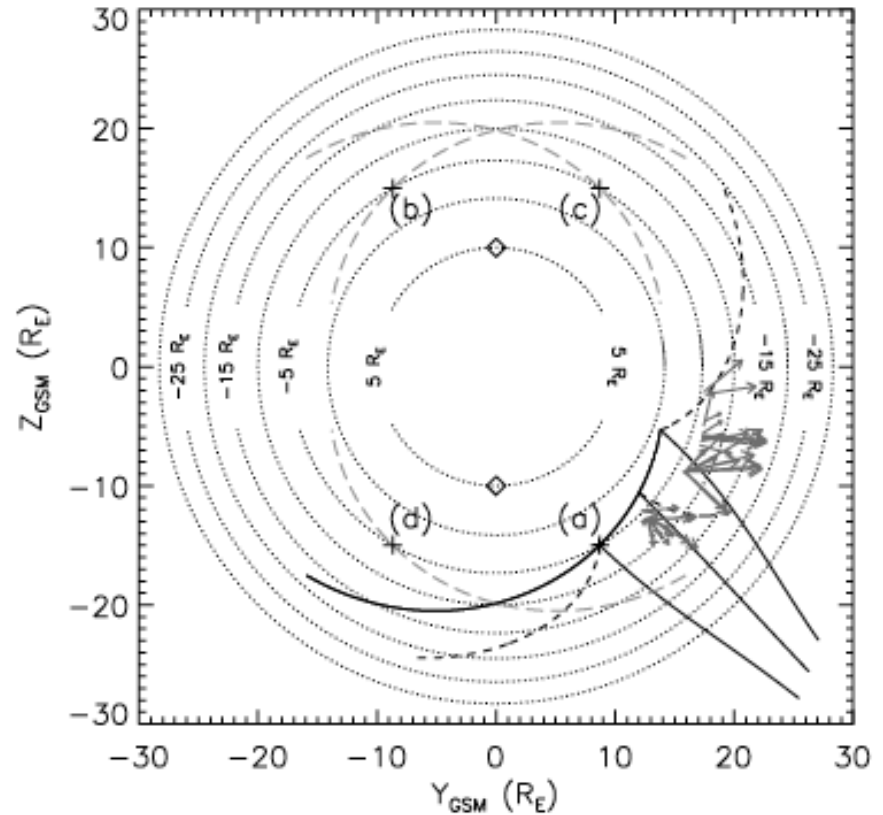
- Standard polarity (positive  $\Rightarrow$  negative; **X**): predominantly in the northern hemisphere
- Reverse polarity (negative  $\Rightarrow$  positive; **O**): predominantly in the southern hemisphere
- Indicative of subsolar reconnection as a generation mechanism (even when there is a dominant IMF By condition, leading to guide-field reconnection [Russell+, 1985])

# FTE: IMF Bz dependence

340 FTEs from ISEE 1 [Kawano & Russell, 1997a]

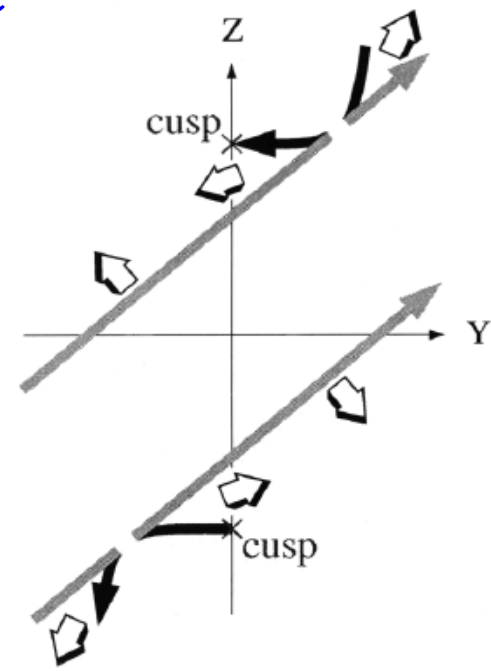
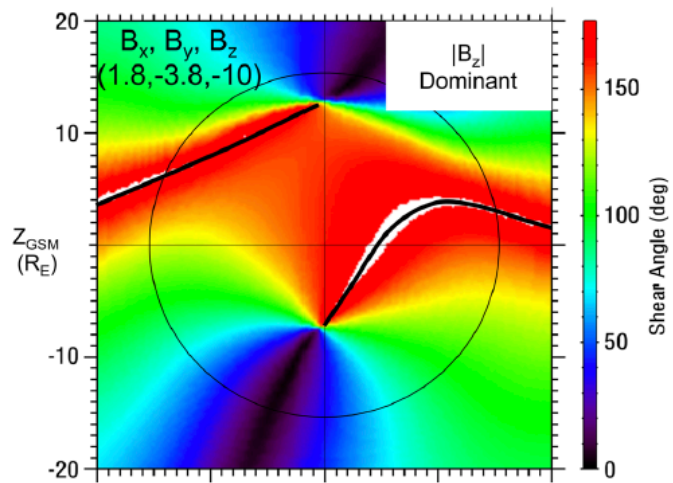
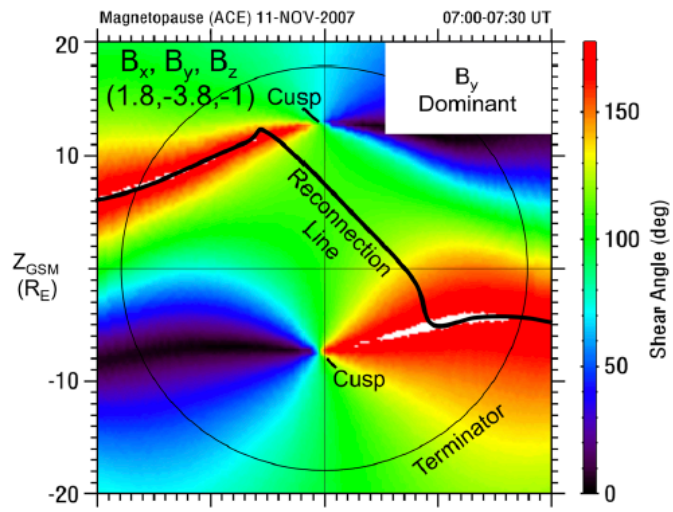
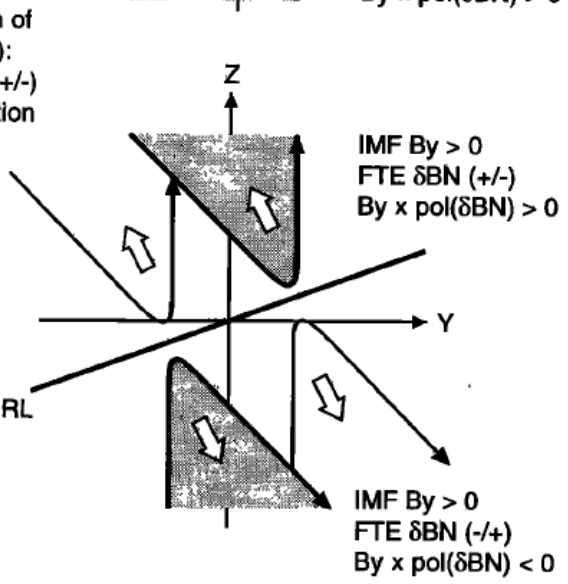
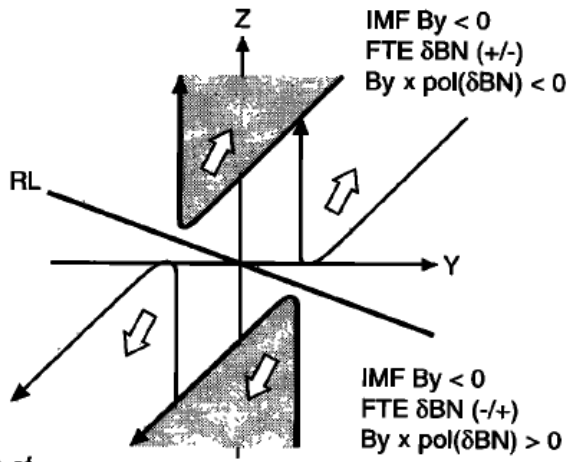


FTEs from Cluster during IMF +Bz [Fear+, 2005]



- Subsolar and pre/post-noon FTEs are observed mainly during southward IMF [Kuo+ 1995; Kawano & Russell, 1997a,b]
- Post-terminator FTEs are associated with strongly northward IMF [Kawano & Russell, 1997a,b]  $\leq$  high-latitude reconnection for IMF +Bz
- FTE event from Cluster shows an tailward/equatorward motion during IMF +Bz

# FTE: IMF By dependence

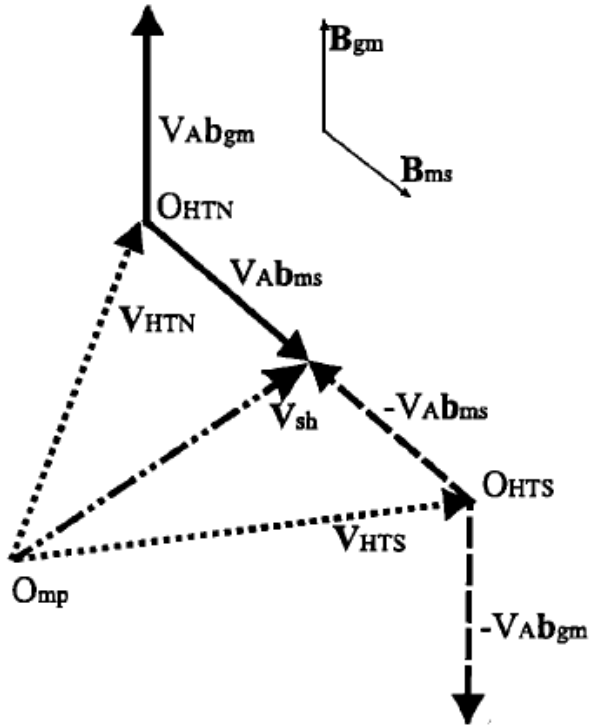


**$B_y$  dependence for strong IMF  $+B_z$  [Kawano & Russell, 1997b]**

- Southward and slightly northward IMF: Most of events are explained by a tilted subsolar component RX
- More northward IMF: Cusp reconnection explains polarities and IMF  $B_y$  dependence.

**$B_y$  dependence during IMF  $-B_z$  [Kawano & Russell, 1997a; left] [Fuselier+, 2016; right]**

# FTE: Motion – Magnetosheath Flow Effect

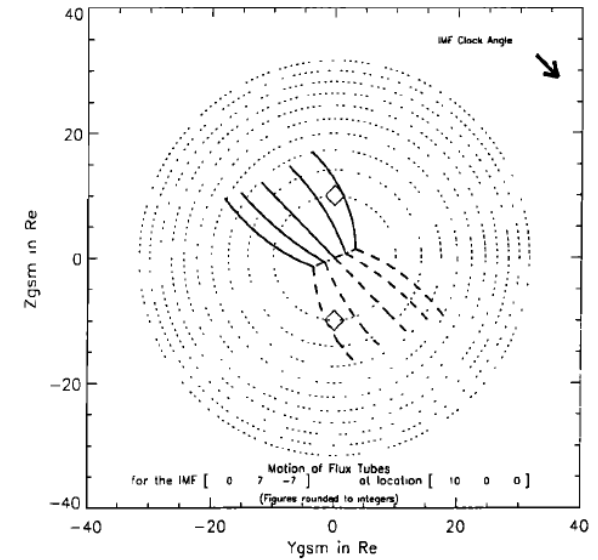
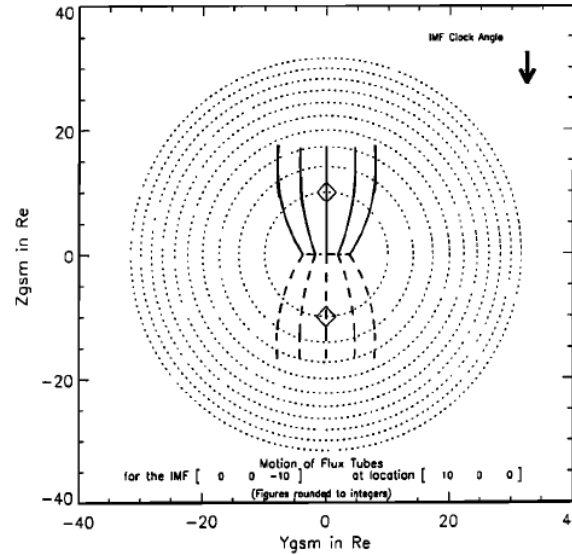


$$V_{HTN} = V_{SH} - V_A \hat{b}_{SH}$$

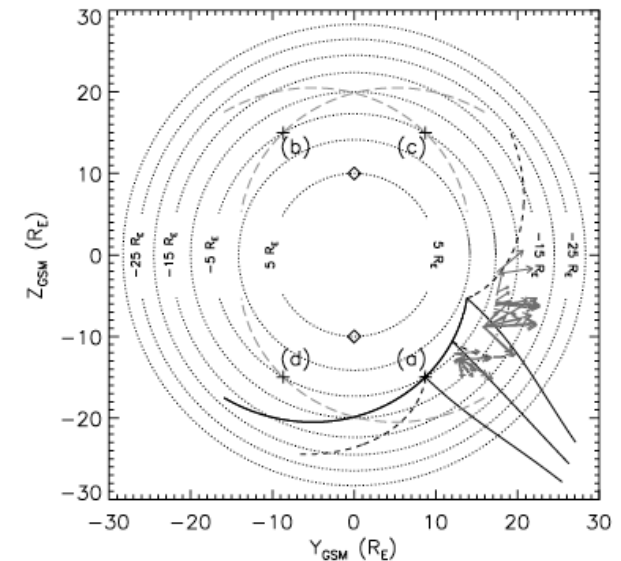
$$V_{HTS} = V_{SH} + V_A \hat{b}_{SH} \quad [\text{Cowley \& Owen, 1989}]$$

- 118 FTE statistics from Cluster show consistency in both direction and speed with either  $V_{HTN}$  or  $V_{HTS}$  calculated from the Cooling model [Fear+, 2007]

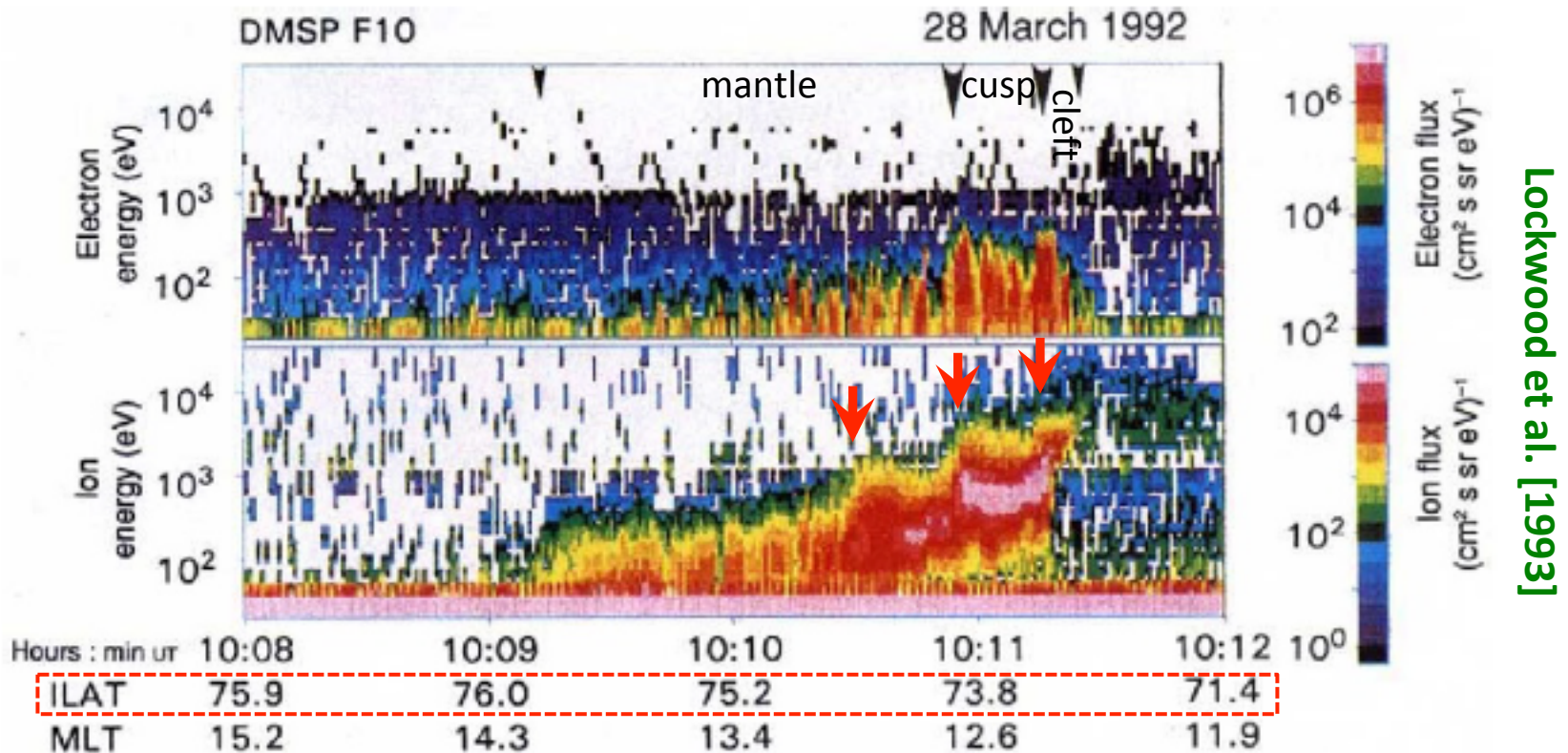
Motion of FTEs [Cooling+, 2001]



Motion of FTEs for IMF +Bz [Fear+, 2005]

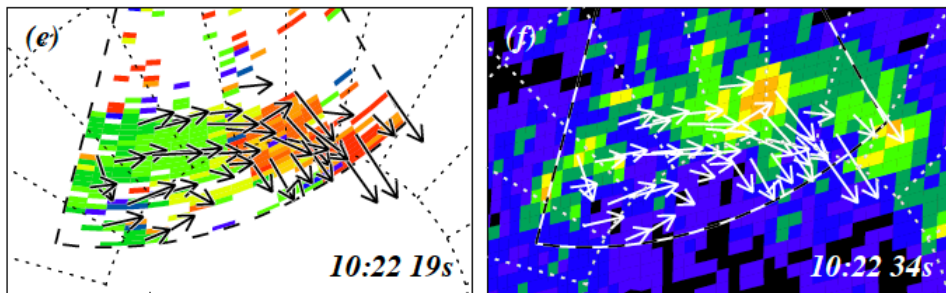
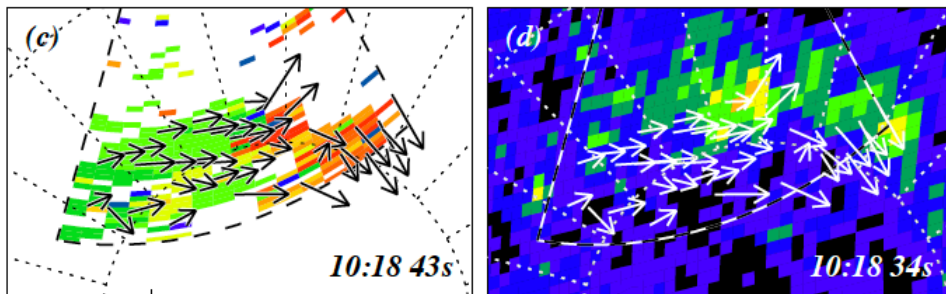
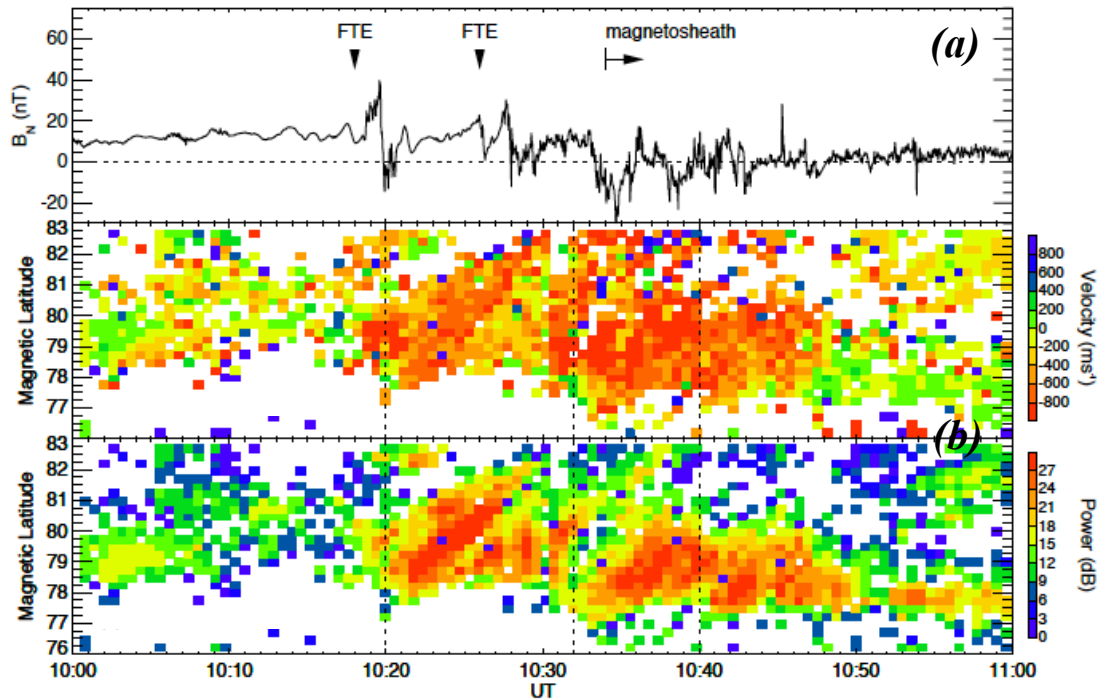


# FTE: Cusp responses



- Steady-state reconnection leads to dispersion pattern of precipitating ions in the cusp region (**lowest time of flight from X, for highest energy ions**): For subsolar RX, decrease in ion energies with latitude
- Pulses in reconnection cause discrete steps (red arrows) in ion dispersion
- Evidence for the fact that reconnection takes place in a series of bursts, therefore, producing FTEs

# FTE: Ionospheric Responses



Neudegg et al. [2001]

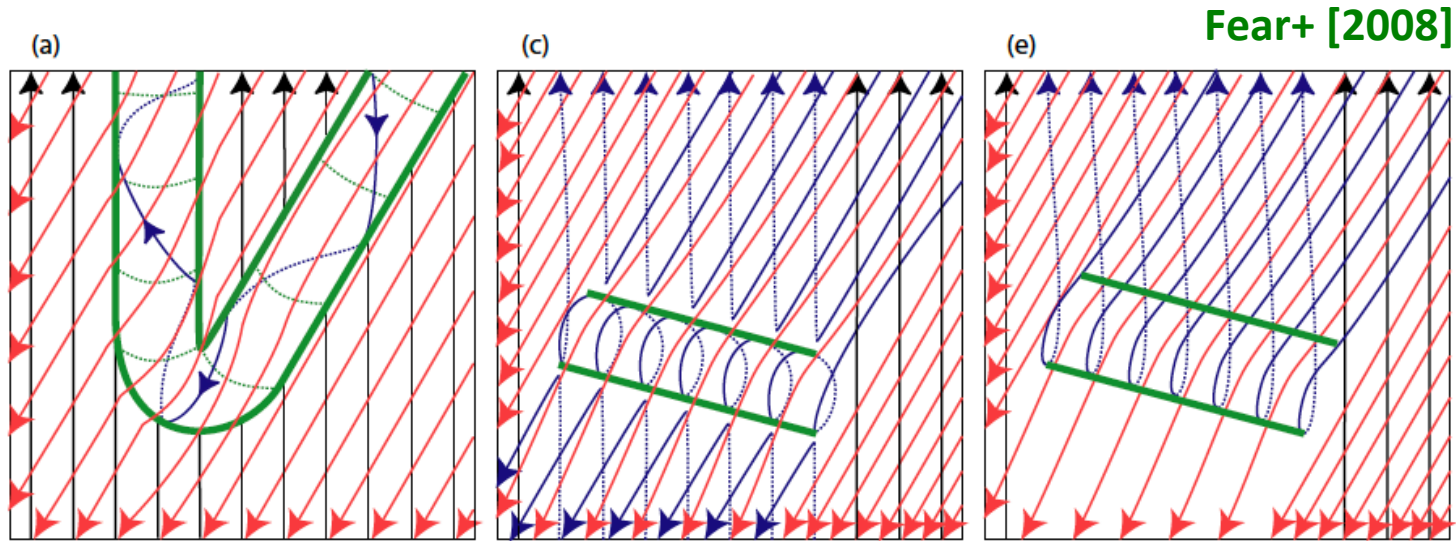
- At the footprints of newly opened magnetic field lines
- Optically, as Poleward Moving Auroral Forms (PMAF) [Sandholt+ 1986; 1992]
- In radar, as Pulsed Ionospheric Flows or Poleward Moving Radar Auroral Forms [Provan+ 1998; McWilliams+, 2000]
- Conjugate studies between In-situ and ground-based observations [Elphic+ 1990; Amm+, 2005; Wild+ 2005; 2007]
- **Neudegg+ [2001]: In-situ (a) + Radar (b) + Optical (c-f) conjunctions**

[Courtesy to R. Fear]

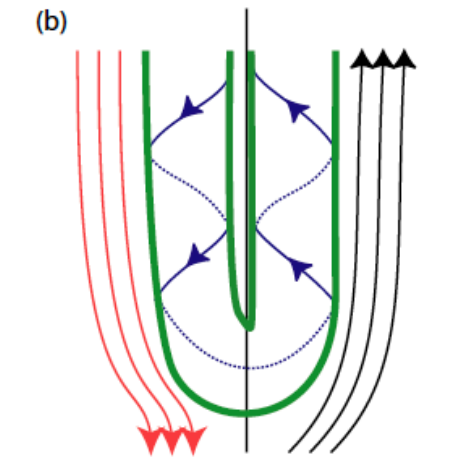
# Outline

1. FTE: general knowns
2. Reconnection-based FTE models
3. New findings on FTE after MMS
4. Velocity-shear-induced FTE

# FTE: Other Reconnection-based Models

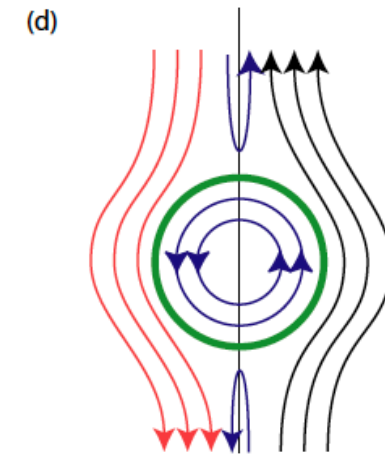


Fear+ [2008]

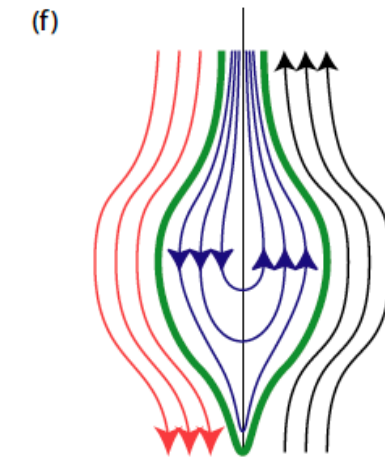


Elbow-shaped flux  
bundle FTEs

Russell & Elphic [1979]

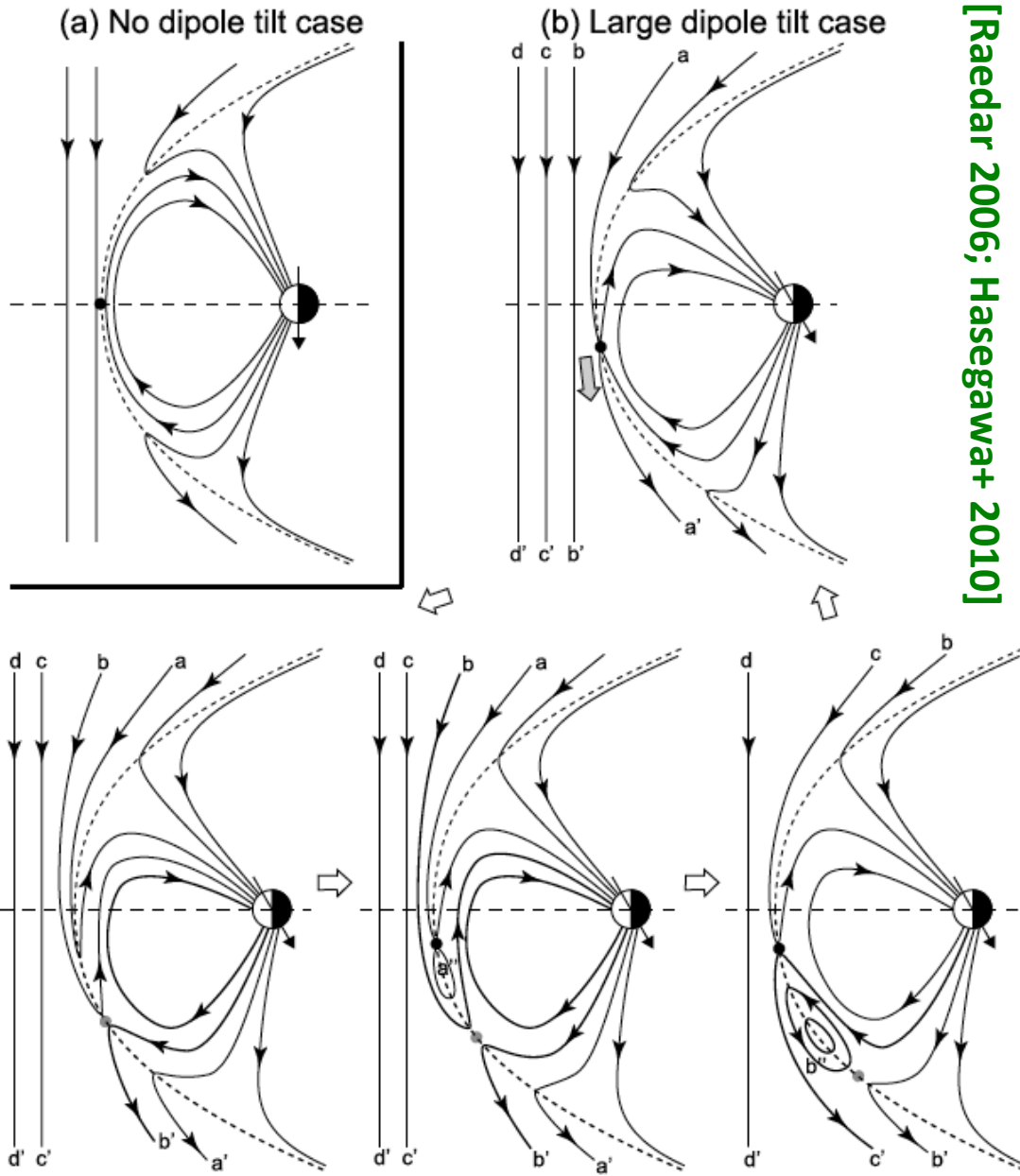


Multiple X-line FTEs  
Lee & Fu [1985]



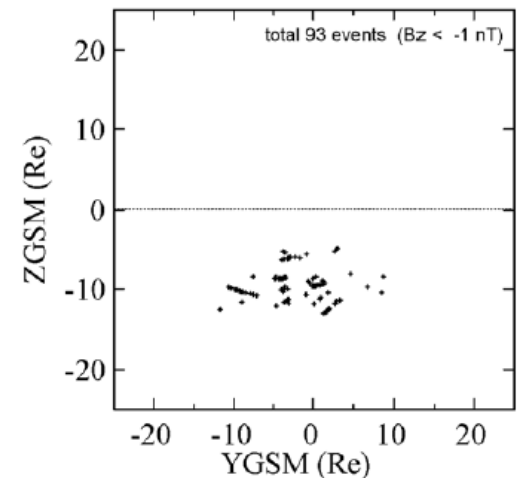
Single X-line FTEs  
Southwood [1988]  
Scholer [1988]

# FTE: Seasonal dependence (SMXR model)

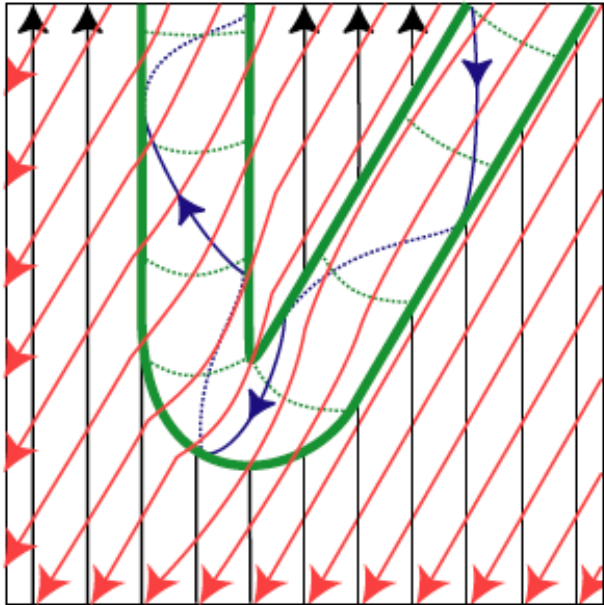


[Raedar 2006; Hasegawa+ 2010]

- In presence of dipolar tilt, FTEs are formed by **sequential multiple X-line reconnection (SMXR)**
- FTEs move preferentially to the **winter hemisphere**
- SMXR: not present in all related simulation works
- Korotova+ [2008] showed FTEs detected by Interball-1 around June solstice in 1996-1999 are found exclusively in winter hemisphere



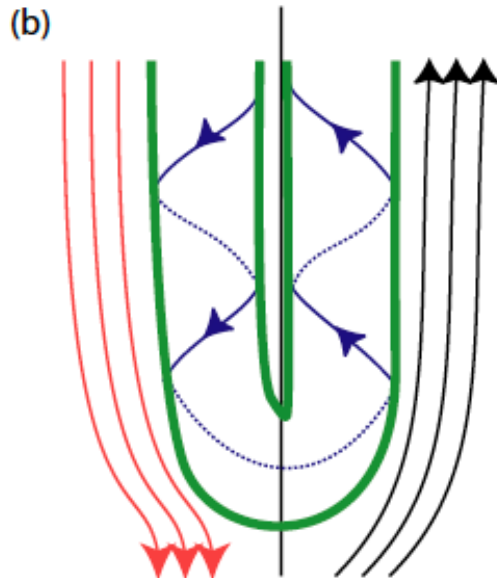
# FTE: Signatures of Elbow-shaped flux-bundle FTEs



Formed by localized patchy reconnection

## **B topology:**

- Topologically open
- The spiral magnetic field lines connect the magnetosheath magnetic field to either the northern or southern high-latitude ionosphere
- Their magnetosheath and magnetospheric ends connect through a circular hole (with a diameter of  $\sim 1 R_E$ ) on the magnetopause



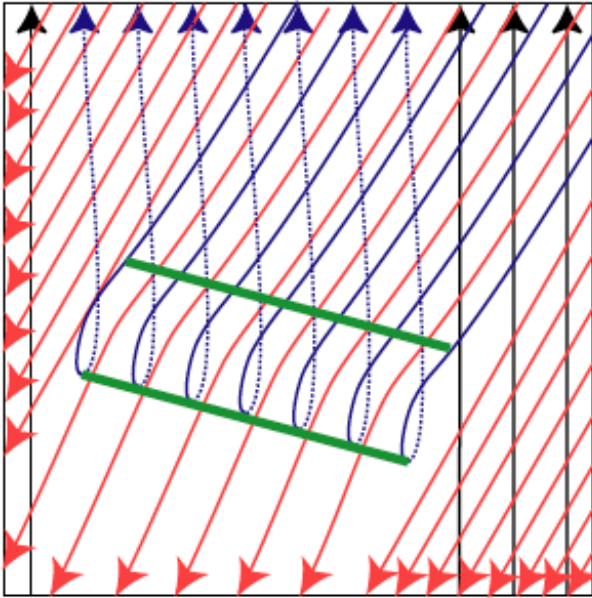
## **Extent:**

- Having narrow azimuthal (dawn-dusk) extents

## **Particle signature:**

- Bidirectional electrons at the edge of FTEs
- Mostly unidirectional ions in the rearward edge of the FTE [Varsani+, 2014]
- Hot and more isotropic electrons in the FTE core

# FTE: Signatures of Single X-line Model



Via transient increases in the reconnection rate

## **B topology:**

- Topologically open; no helical flux rope
- May contain a core guide field
- The newly reconnected magnetic field lines simply connect the magnetosheath to either the northern or southern hemisphere.

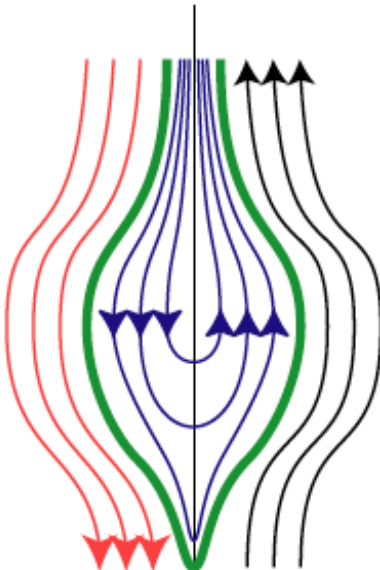
## **Extent:**

- Can extend azimuthally over many  $R_E$

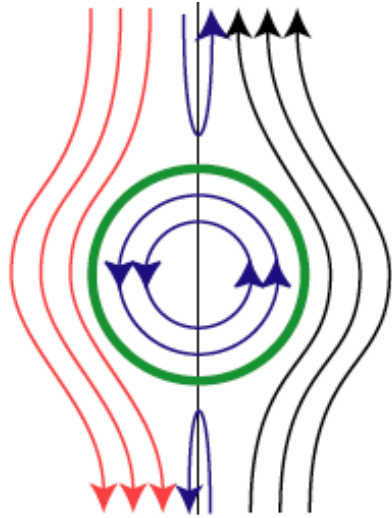
## **Particle signature:**

- Reconnection jets flow away from the X-line on the edges of FTEs
- Thermalized plasma populate within the core
- The particle signatures similar to Elbow-shaped FTEs
- Lockwood and Hapgood [1998]: continuous variation in the ion distribution function between the event core (reconnected earlier) and the draped field lines (reconnected later)

(f)



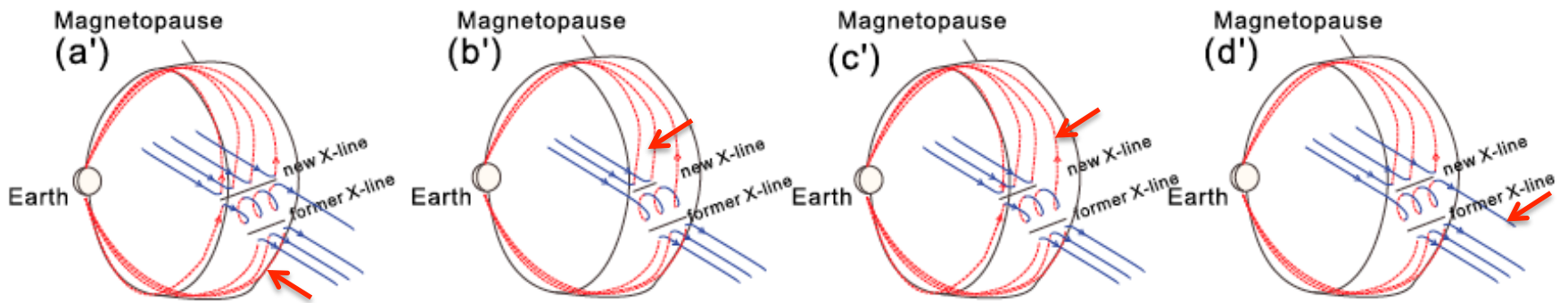
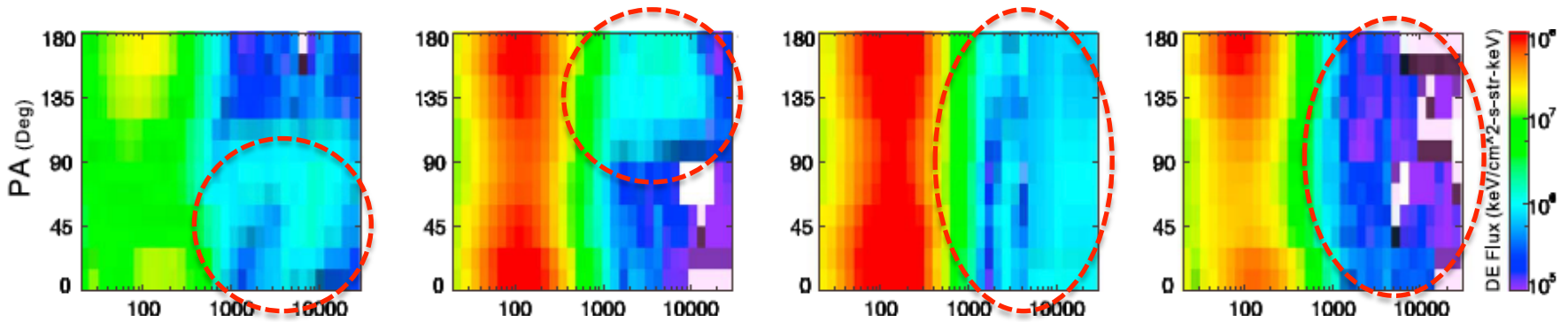
# FTE: Signatures of Multiple X-line Model - 1



Via simultaneous or sequential multiple X-lines

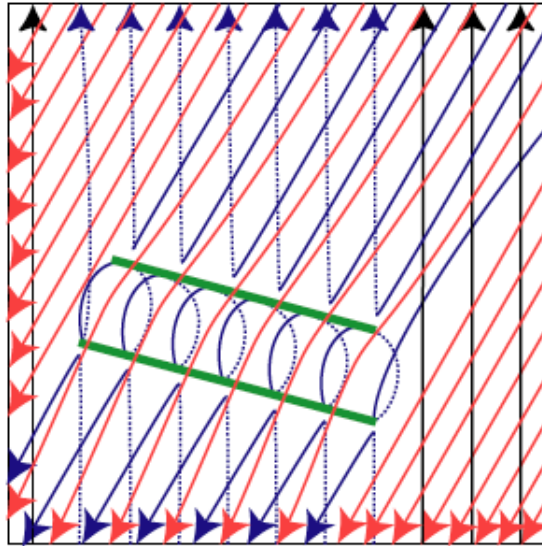
**B topology:**

- Possibly topologically closed
- Mixed magnetic field topologies, e.g., open field lines connecting the northern or southern hemisphere to the magnetosheath, closed field lines connecting both hemispheres, and purely magnetosheath fields [Pu+ 2013; Zhong+, 2013]



[Pu+ 2013]

# FTE: Signatures of Multiple X-line Model - 2



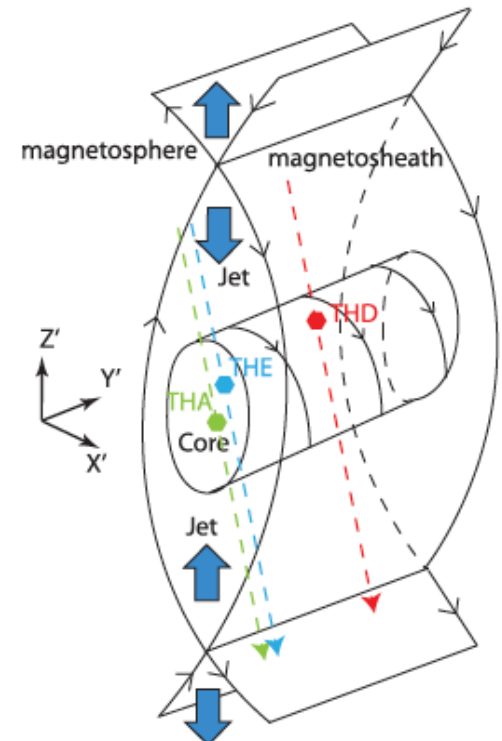
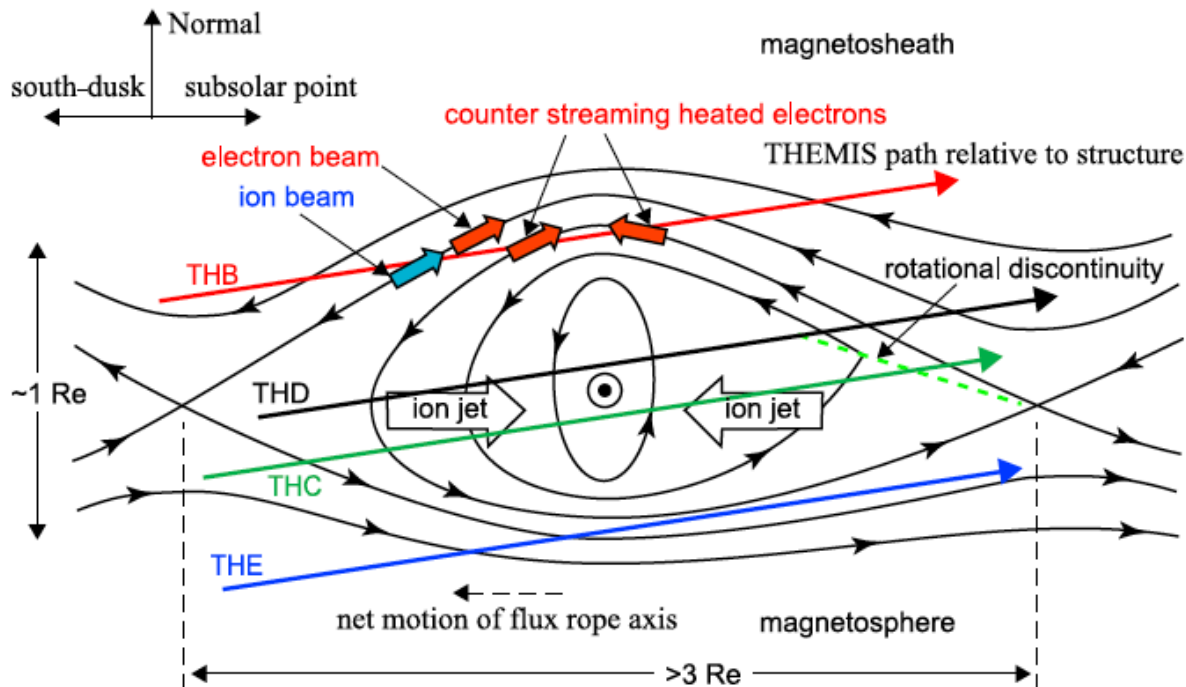
Via simultaneous or sequential multiple X-lines

**Extent:**

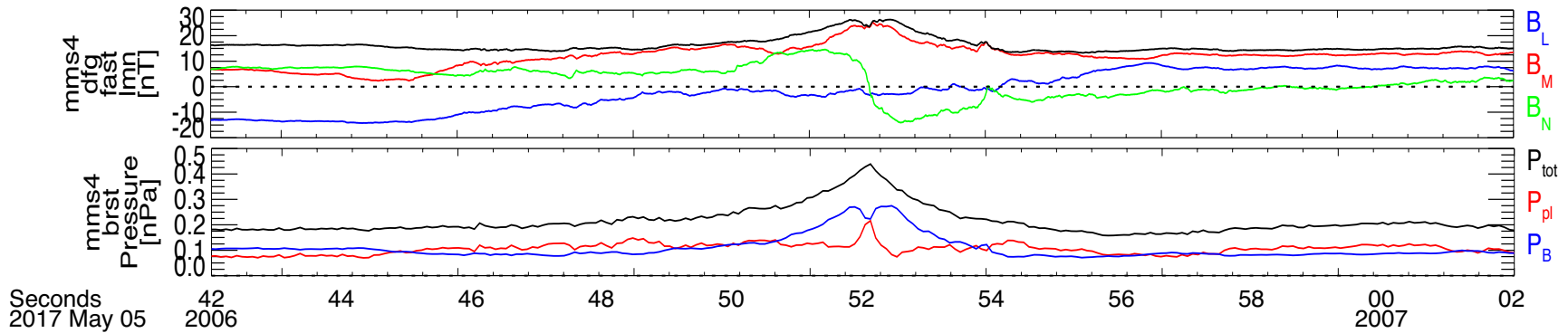
- Can extend azimuthally over many  $R_E$

**Particle signature:**

- Two ion jets converging toward the center of such FTEs [Hasegawa+, 2010; Øieroset+, 2011]
- Heated magnetosheath electrons flowing both parallel and antiparallel to B [Hasegawa+, 2010]



# FTE: Crater FTEs

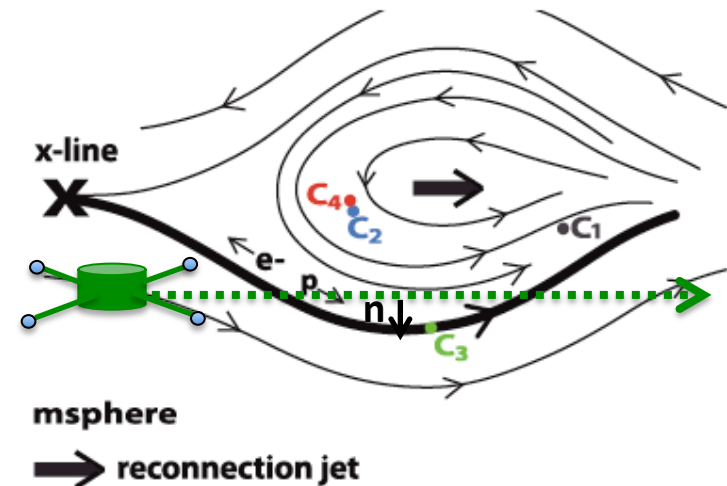
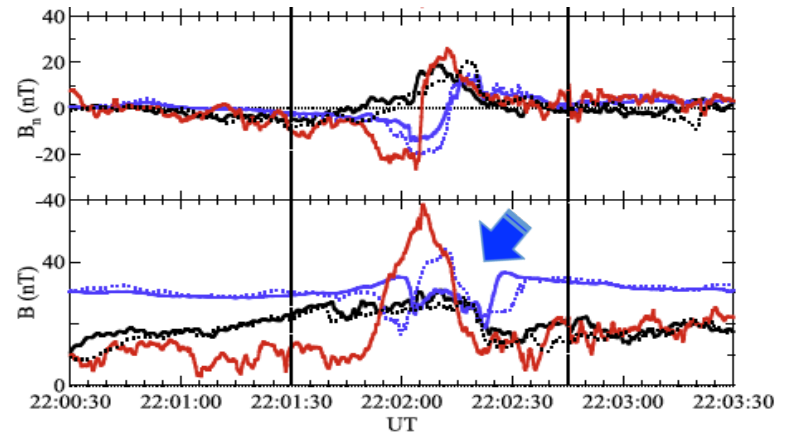


## More complex shape in $|B|$ enhancement:

- 'M'-shaped: central depression in  $|B|$
- 'W'-shaped: strong core bounded by weak  $|B|$

## Scenarios:

- Pressure pulses-causing transient relocation of the spacecraft across the boundary layer with respect to an FTE [Sibeck & Smith, 1992; Owen+, 2008]
- Encounters with the separatrix resulting in the crater-like  $B$  variations with bipolar  $B_n$  across the event [Farrugia+, 2011]



[Hwang+ in prep]

[Sibeck+, 2008]

[Farrugia+, 2011]

# FTE: Multi-spacecraft observations before MMS

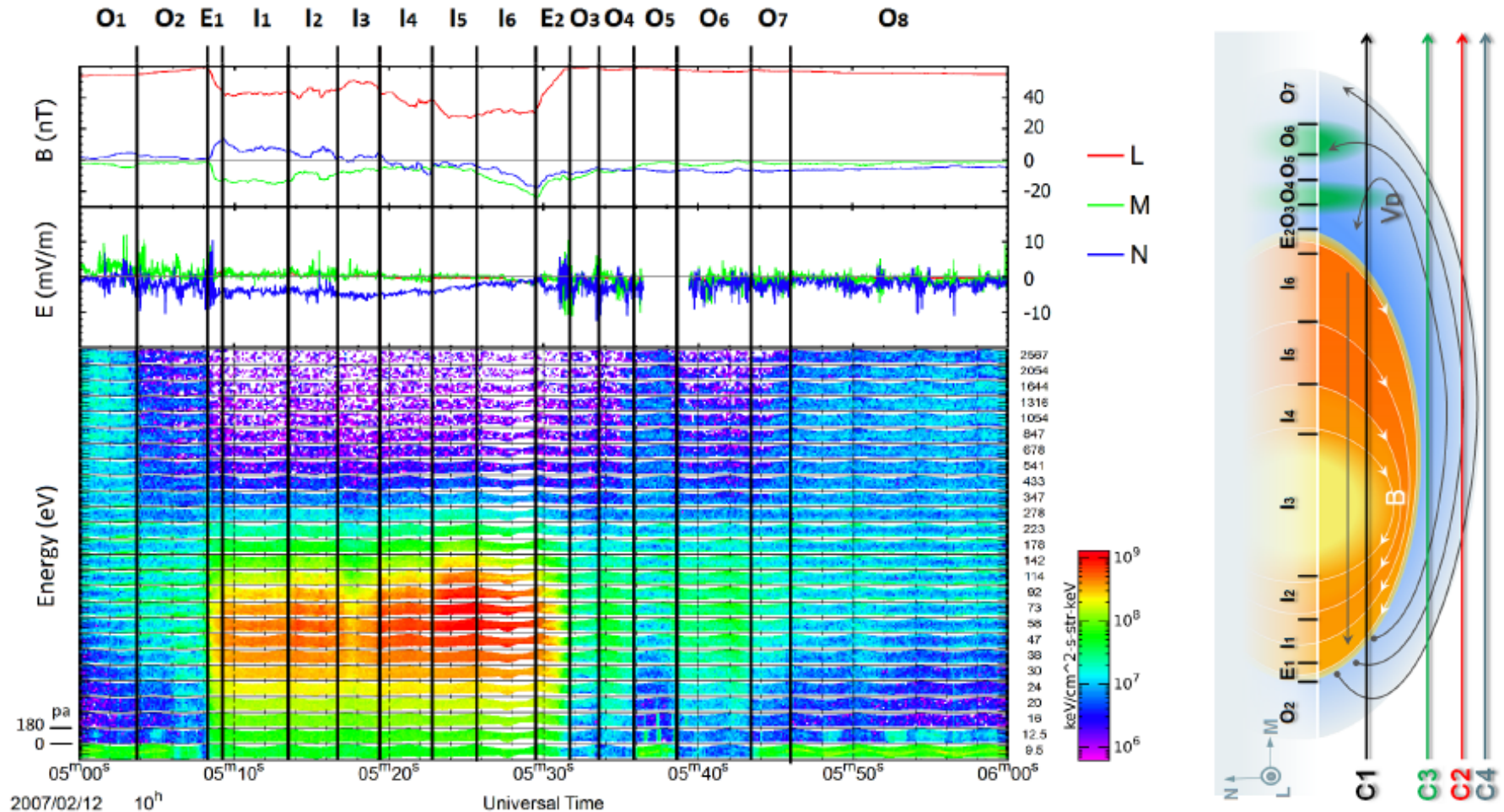
## Distinguishing among different models:

- **Fear et al. [2008]** used tetrahedral **Cluster** observations to describe an FTE with a much larger azimuthal than north-south extent, which is inconsistent with the elbow-shaped flux tube model.
- **Dunlop et al. [2005]** presented **Cluster** and **TC-1** observations of a pair of FTEs propagating northward and southward away from the reconnection site, consistent with single X-line model.
- **Hasegawa et al. [2010]** reported **THEMIS** observation of an FTE between two converging jets, and therefore suggested multiple X-line model (**Grad-Shafranov reconstruction** using multi-s/c measurements).
- **Farrugia et al. [2011]** reported a single X-line crater FTE with multiple layers on the basis of their magnetic, electric, and plasma signatures from the four **Cluster** spacecraft.

## Magnetic topology using B-field and electron measurements on improved temporal resolution:

- **Owen et al. [2001]** used Cluster-FGM/PEACE observations to define the magnetic field connectivity of the substructure of FTEs inferred from the magnetic field and electron signatures.
- **Øieroset et al. [2011]** presented observations of electrons that were not trapped within the FTE, demonstrating that the event was three-dimensional and had an open magnetic field topology.
- **Pu et al. [2013], Zhong et al. [2013]** used energy-dependent electron pitch angle distributions to show mixed magnetic field topologies of a multiple X-line FTE.
- **Varsani et al. [2014]** identified the multi-layer interior and surrounding structures of a crater FTE based on the electron pitch angles using 125 ms observations of Cluster-PEACE measurements assuming that the electrons were gyrotropic.

# FTE: Multi-spacecraft observations before MMS



**Magnetic topology using B-field and electron measurements on high time resolution:**

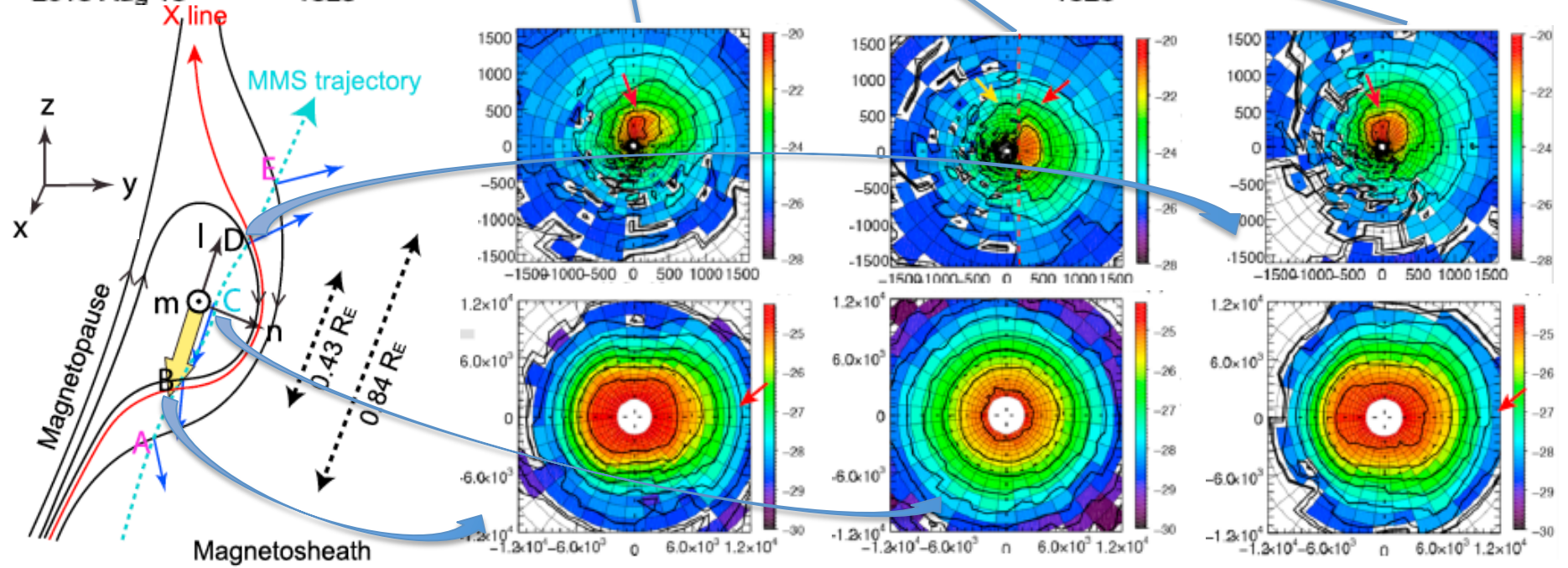
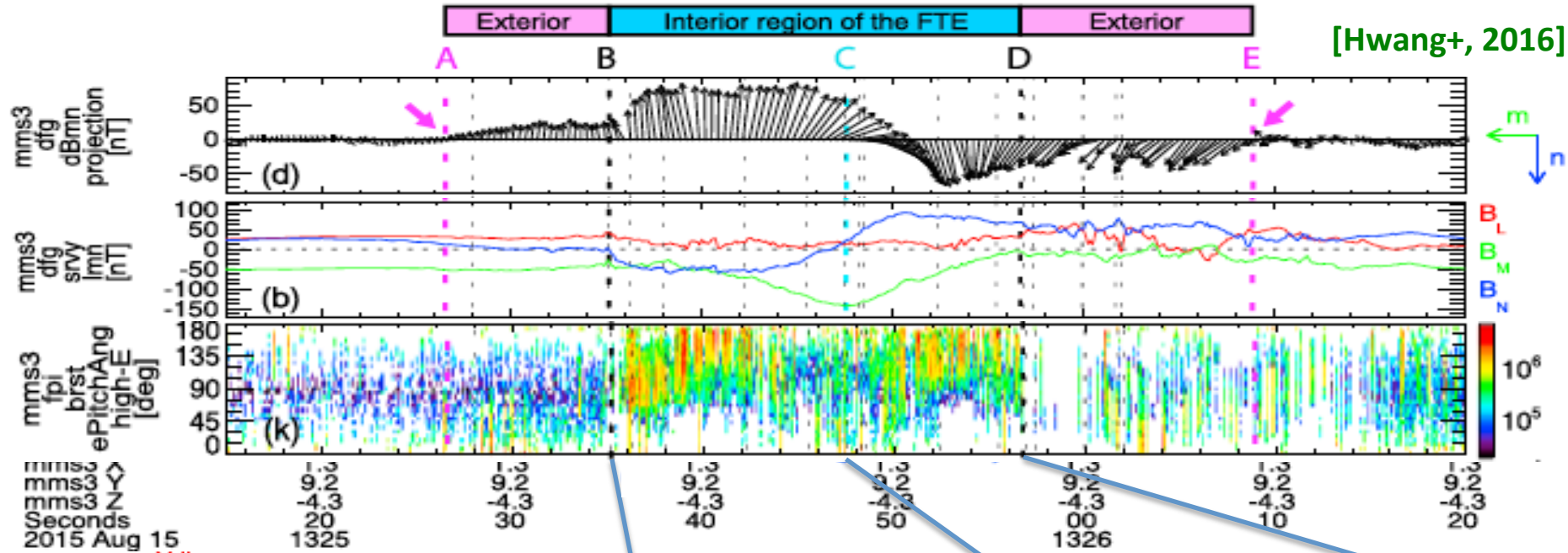
- Varsani et al. [2014] identified the multi-layer interior and surrounding structures of a crater FTE based on the electron pitch angles using 125-ms observations of Cluster-PEACE measurements assuming that the electrons were gyrotropic.

# Outline

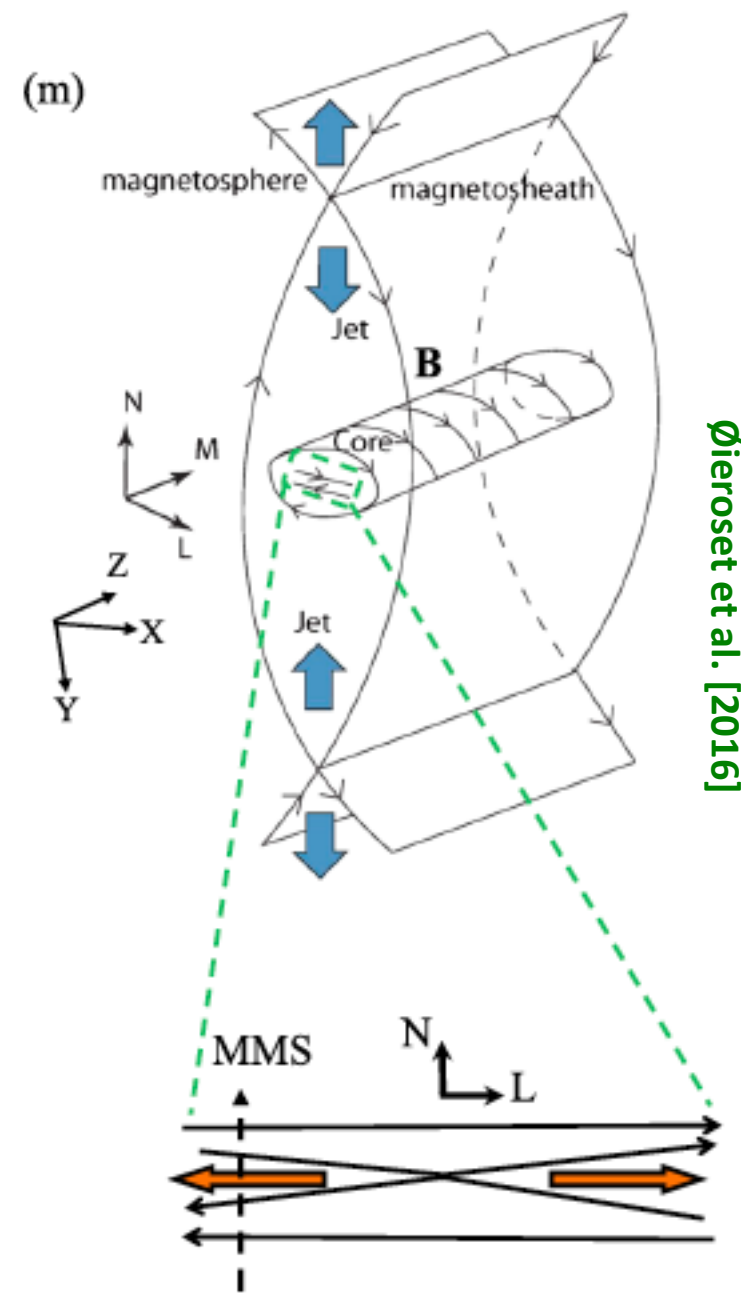
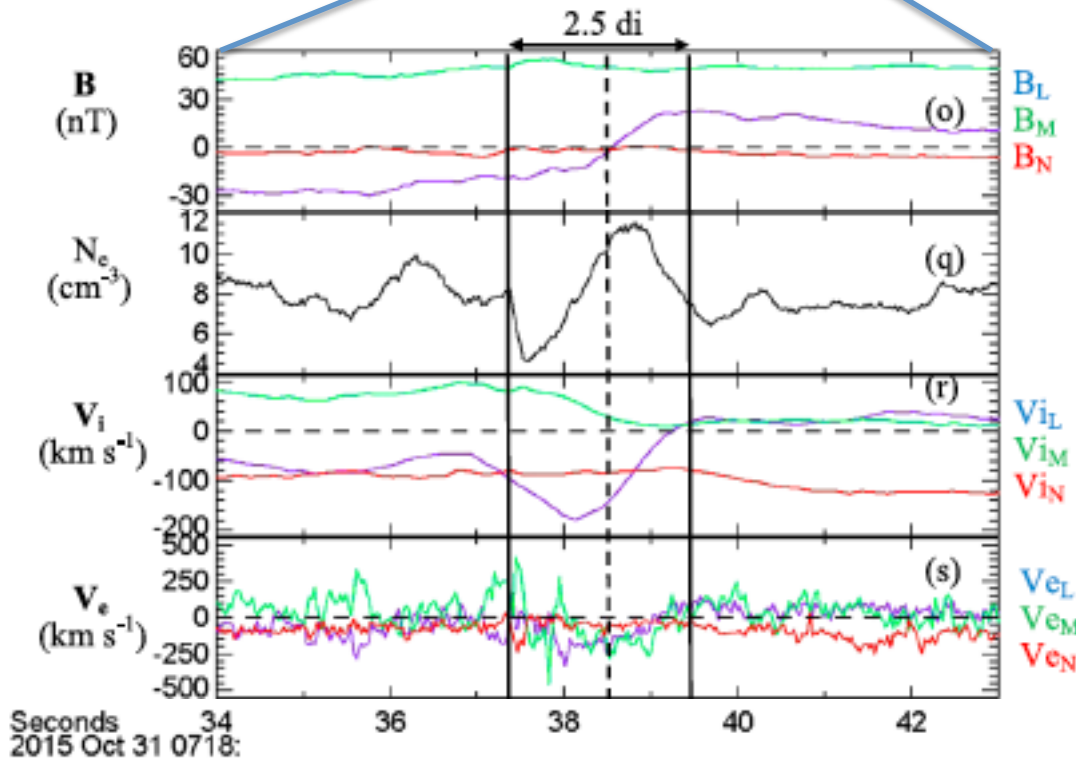
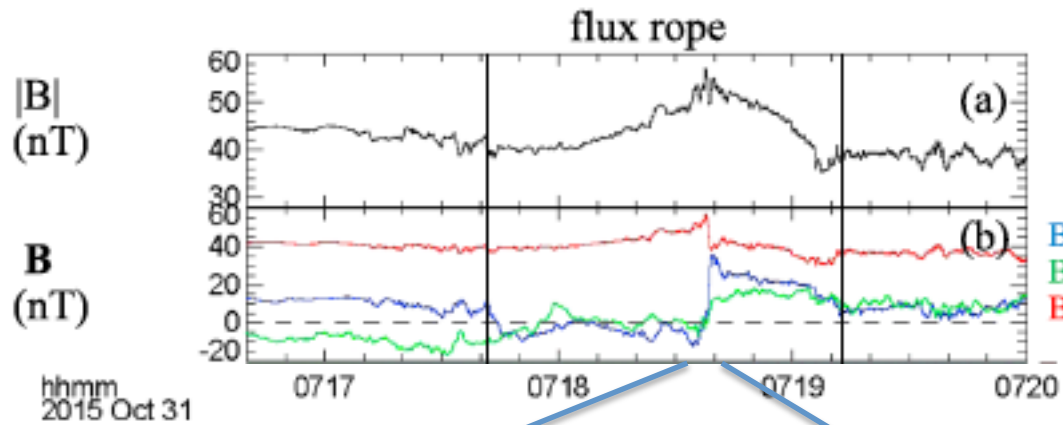
1. FTE: general knowns
2. Reconnection-based FTE models
3. **New findings on FTE after MMS**
4. Velocity-shear-induced FTE

# FTE: After MMS - 1. Substructure

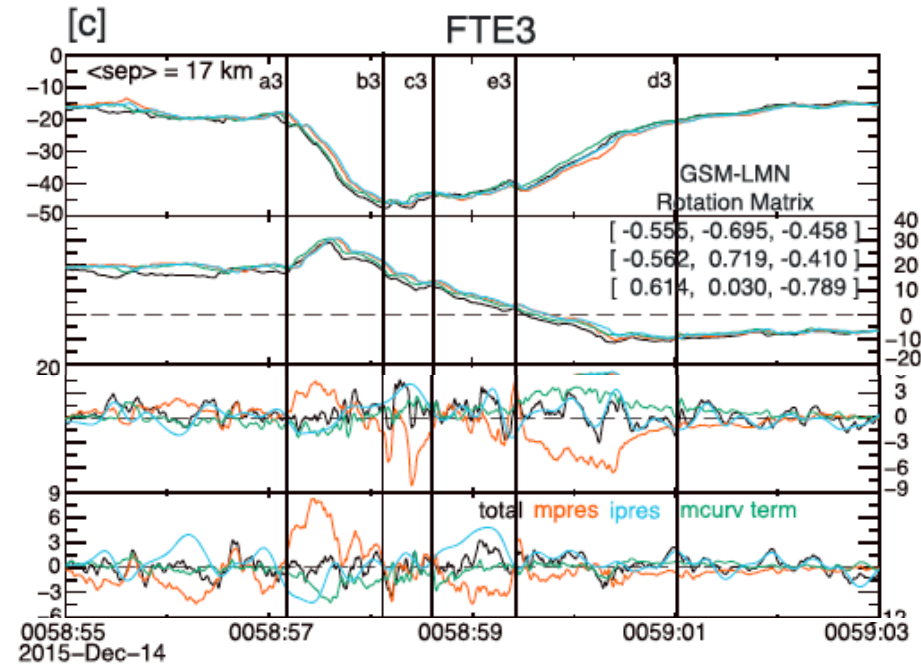
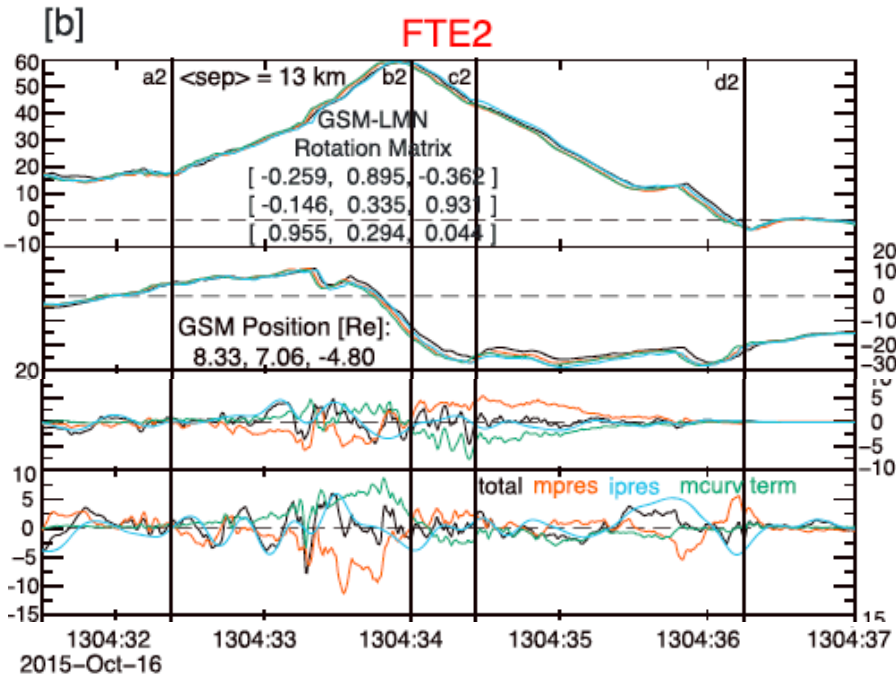
[Hwang+, 2016]



# FTE: After MMS - 1. Substructure



# FTE: After MMS - 2. Force balance



[Zhao et al., 2016]

Force-free flux rope [Lundquist, 1950]:  $\mathbf{J} \times \mathbf{B} = 0$ , i.e.,  $\mathbf{J}$  parallel to  $\mathbf{B}$

$\Rightarrow$  **B curvature (green)** is balanced by **B pressure force (orange)**

- **FTE2 (left)**

- **B curvature** is balanced by **B pressure force**

- **FTE3 (right)**

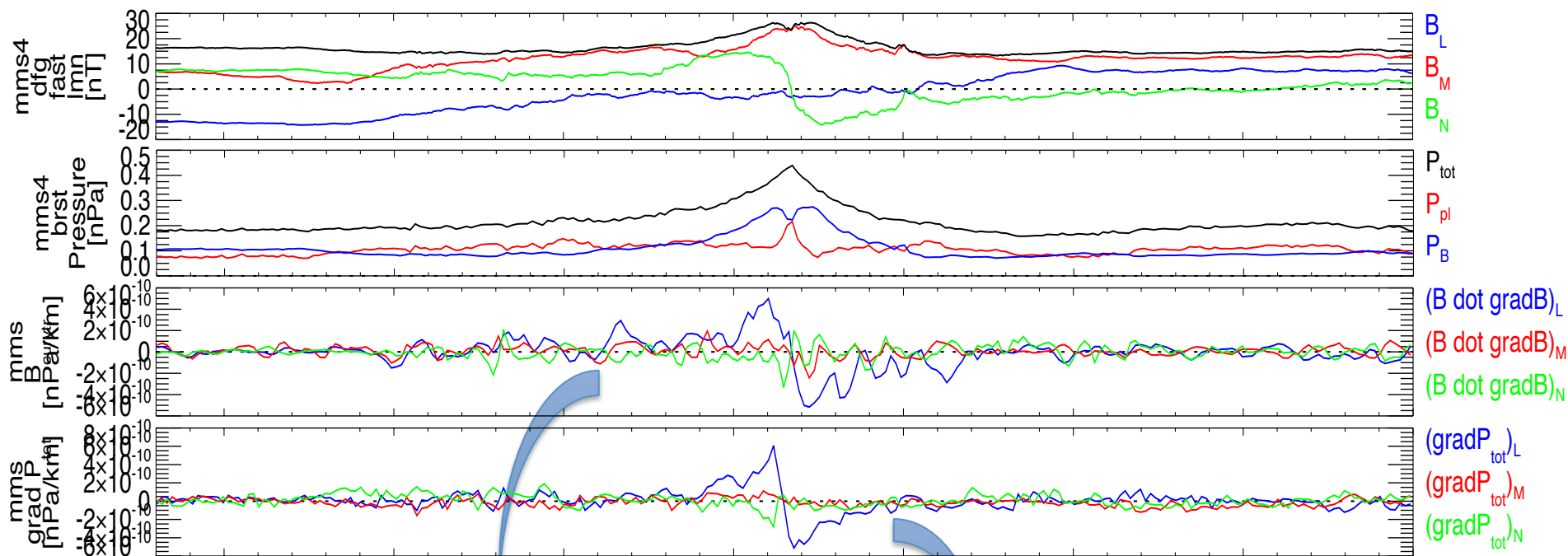
- **B curvature** is NOT balanced by **B pressure force**

- **Ion pressure force (cyan)** is dominant

- Force balanced between  $\mathbf{J} \times \mathbf{B}$  and  $\nabla \cdot \mathbf{P}$

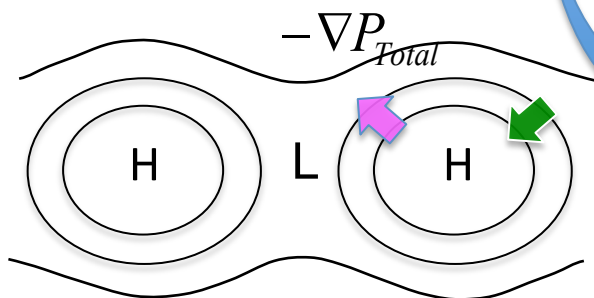
$$\rho \frac{D\mathbf{u}}{Dt} = \mathbf{j} \times \mathbf{B} - \nabla \cdot \mathbf{P}$$

# FTE: After MMS - 2. Force Balance



[Hwang+, in prep.]

Force balance around FTEs:



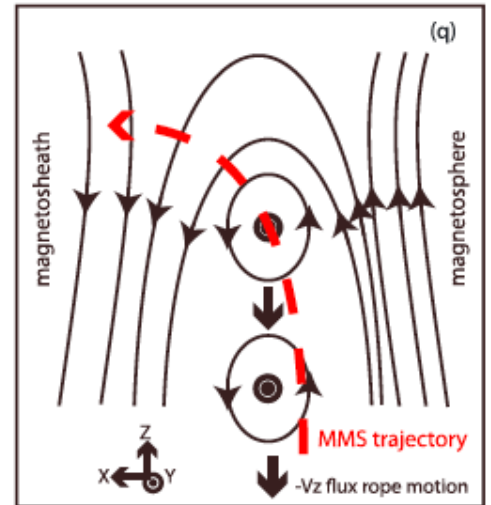
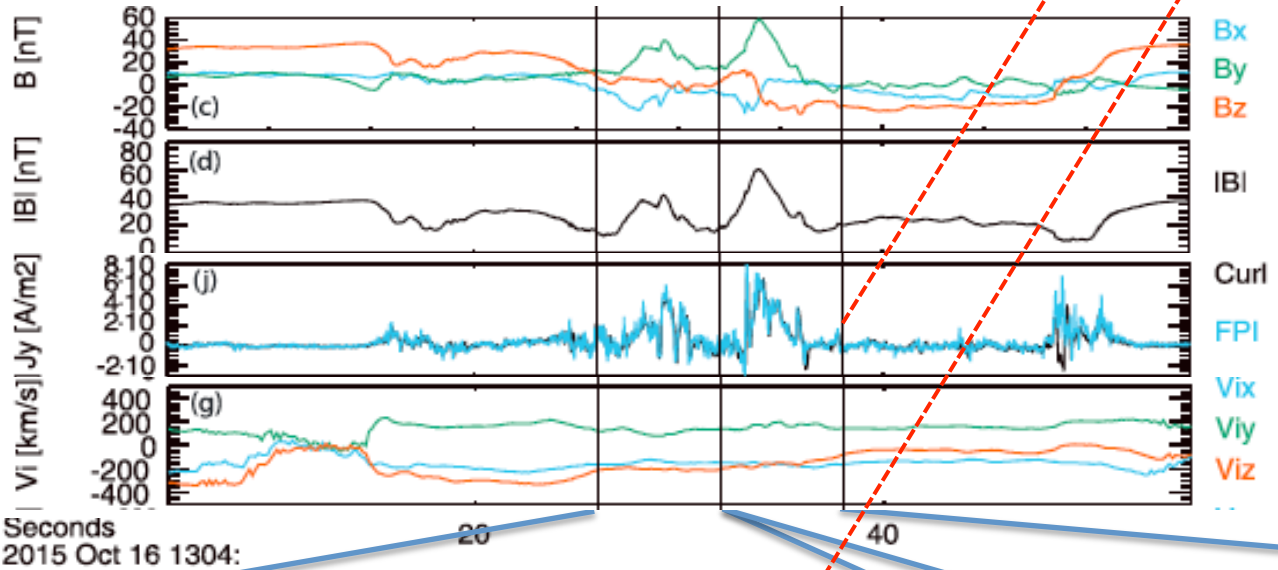
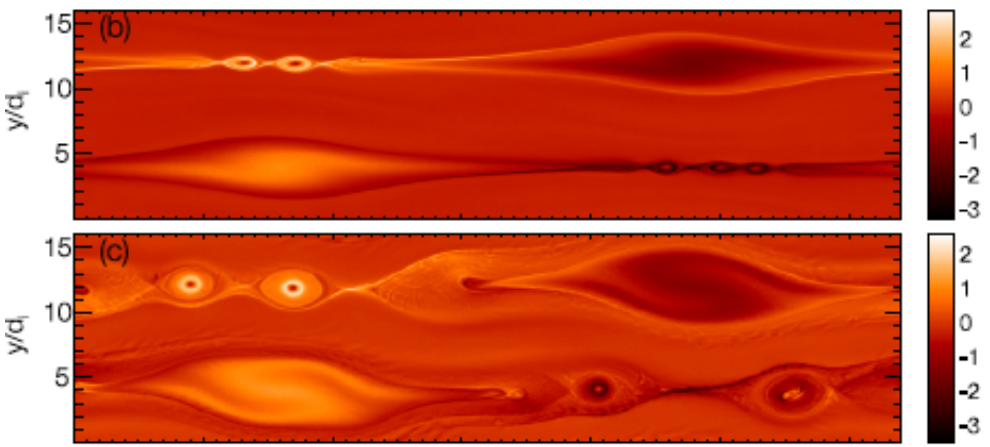
$$-\frac{(\vec{B} \cdot \nabla)\vec{B}}{\mu_0} = -\nabla P_{Total}$$

- **Steady-state FTEs:**
- ✓ Magnetic curvature force is balanced by the **pressure force** [Elphic, 1998; Ieda+, 1998]
- ✓ Not perfectly force-balanced

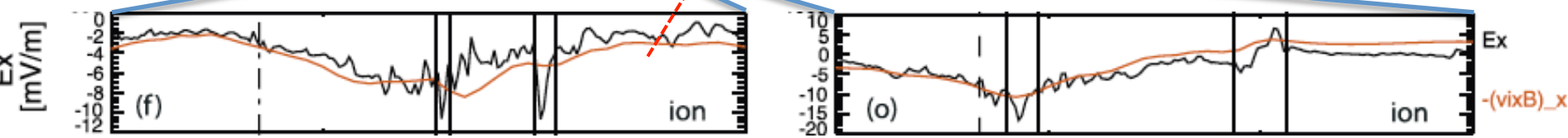
# FTE: After MMS - 3. Small scale FTEs

[Drake+, 2006]

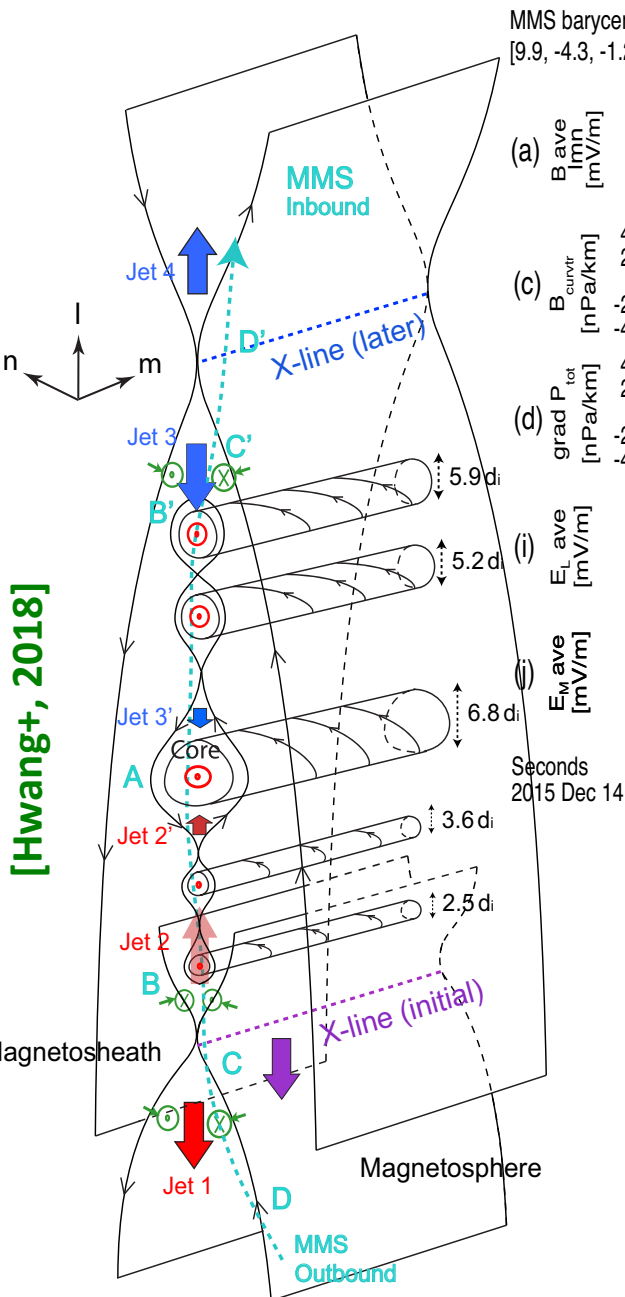
- During  $B_g$ -reconnection, the electron current layers near the magnetic x-line are long => **unstable to the formation of secondary magnetic islands.**
- Ion-scale ( $\sim 7 d_i$ ;  $> 1000$  km) FTEs:
  - ✓ Most likely generated by secondary reconnection
  - ✓ Filamentary current density
  - ✓ Demagnetized ions



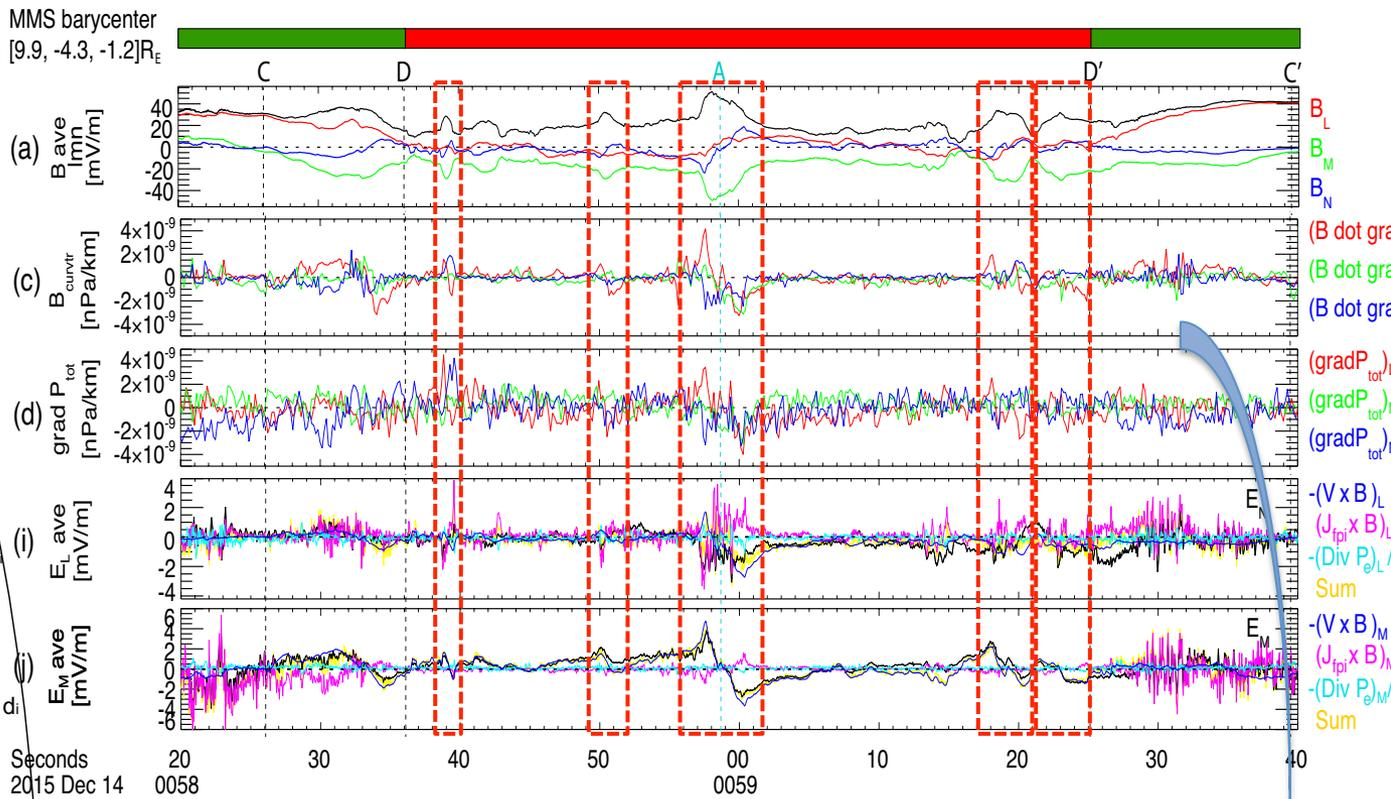
[Eastwood+, 2016]



# FTE: After MMS - 3. Small-scale FTEs



[Hwang+, 2018]

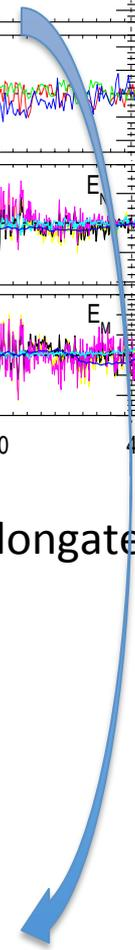


✓ The current sheet between the two X-lines is elongated  
=> **unstable to tearing mode**

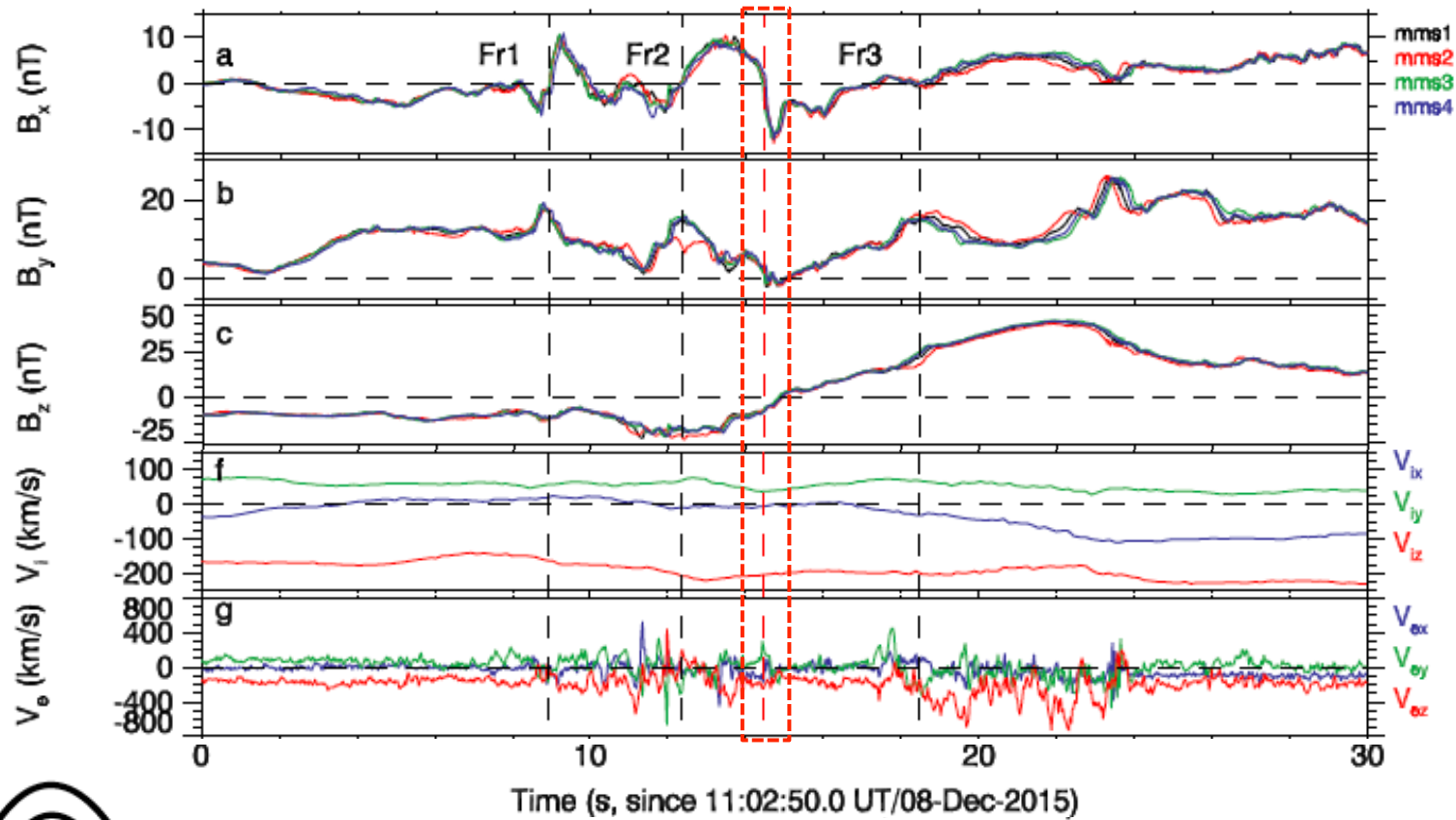
**Scale sizes: 2.5–6.8  $d_i$  (> 187.5 km)**

Supporting observations:

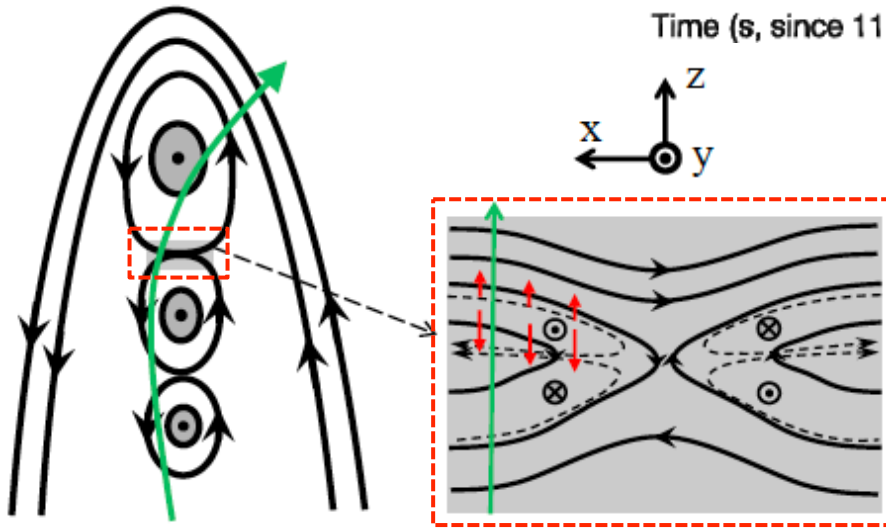
- Converging ion jets toward the FTE center.
- Co-existence of mixed magnetic topology
- **Localized  $B_{curvature}$  mainly balanced by  $Grad_P$**



# FTE: After MMS - 4. Coalescence of small-scale FTEs



[Wang+, 2017]



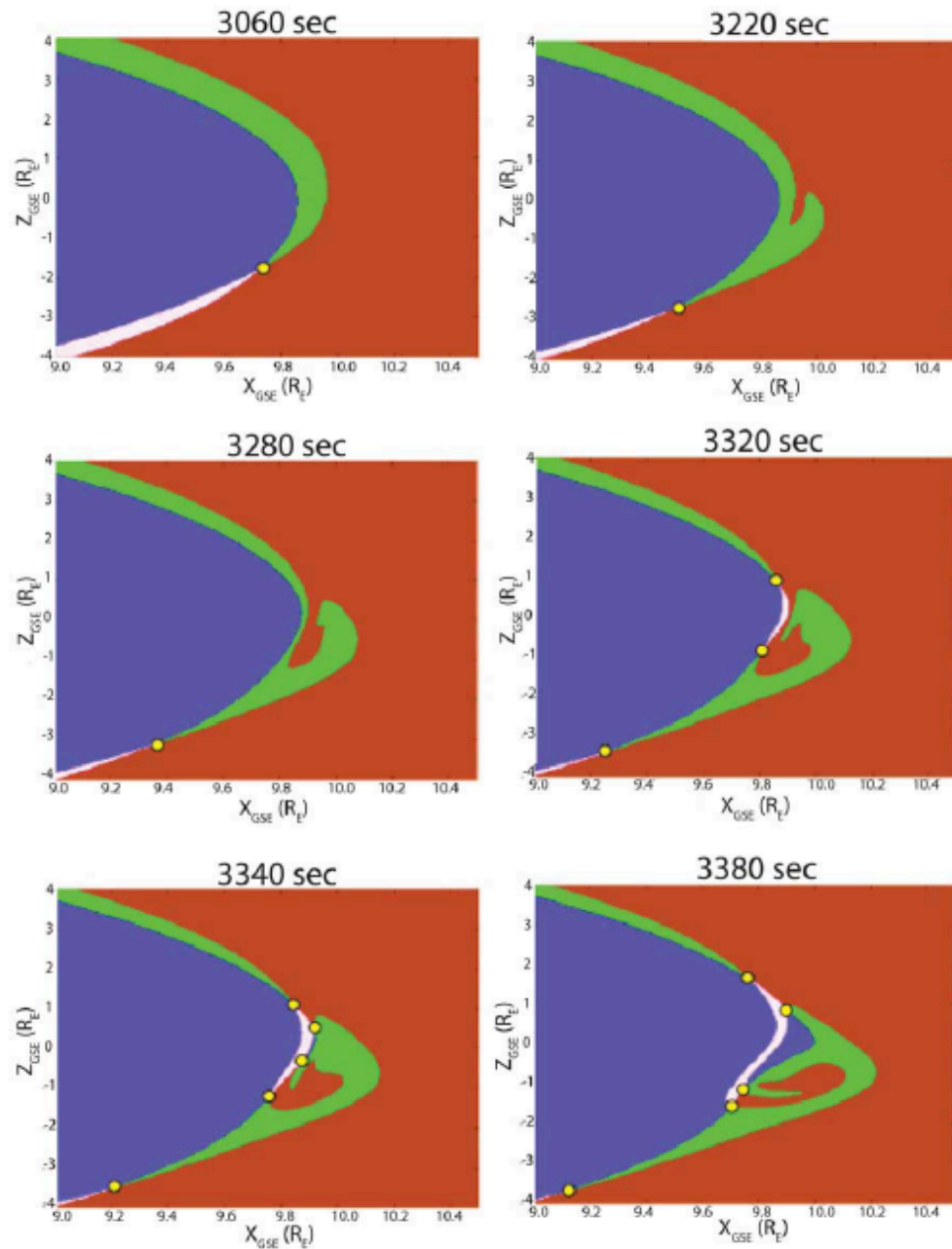
- **Scale sizes:** 1.3–8.6  $d_i$ ; 91–609 km
- **Induced current layer between Fr2 and Fr3:**
  - Carried by electrons
  - $\sim 1 d_i$  thickness

Also, [Zhou+ \[2017\]](#): an electron-scale current layer at the interface of two coalescing macroscopic (with sizes of  $\sim 1 R_E$ ) flux ropes.

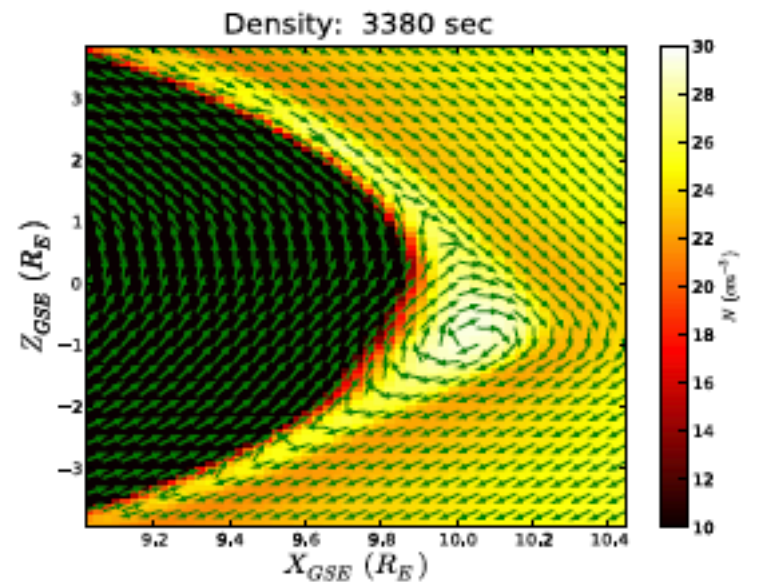
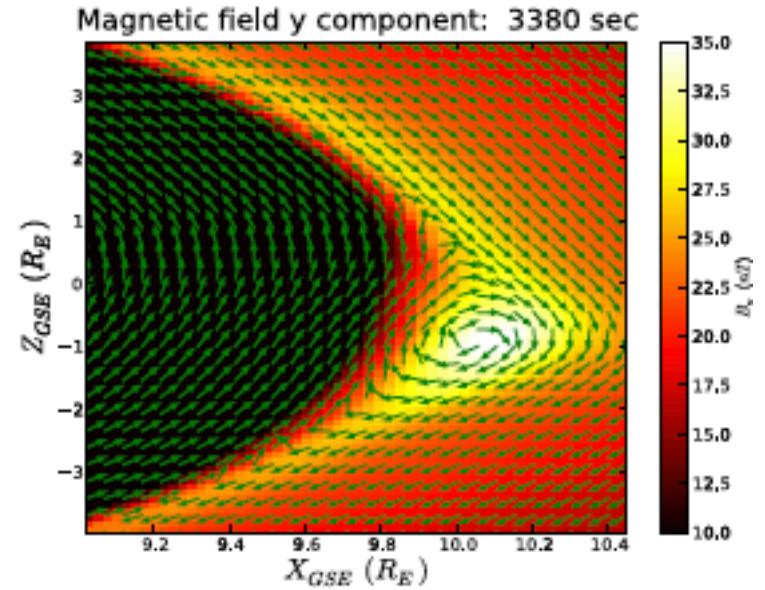
# Outline

1. **FTE: general knowns**
2. **Reconnection-based FTE models**
3. **New findings on FTE after MMS**
4. **Velocity-shear-induced FTE**

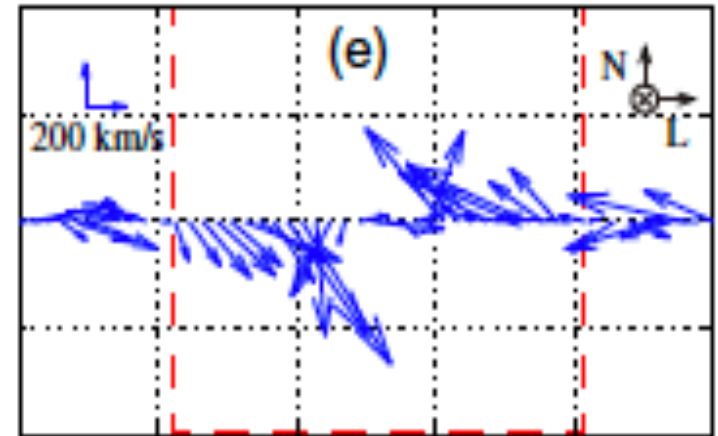
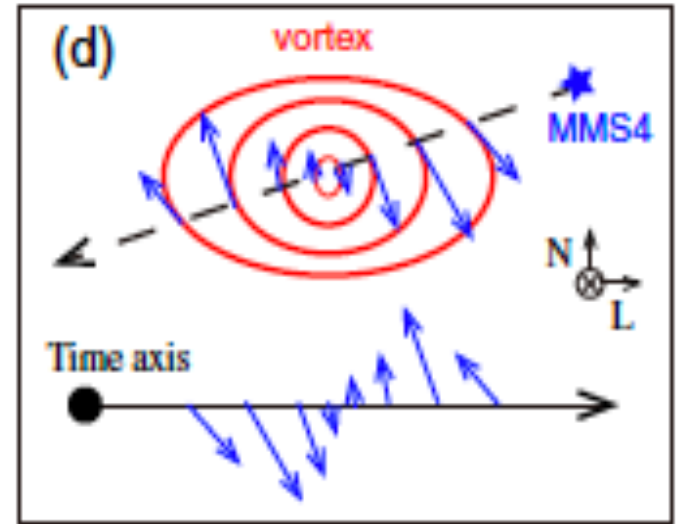
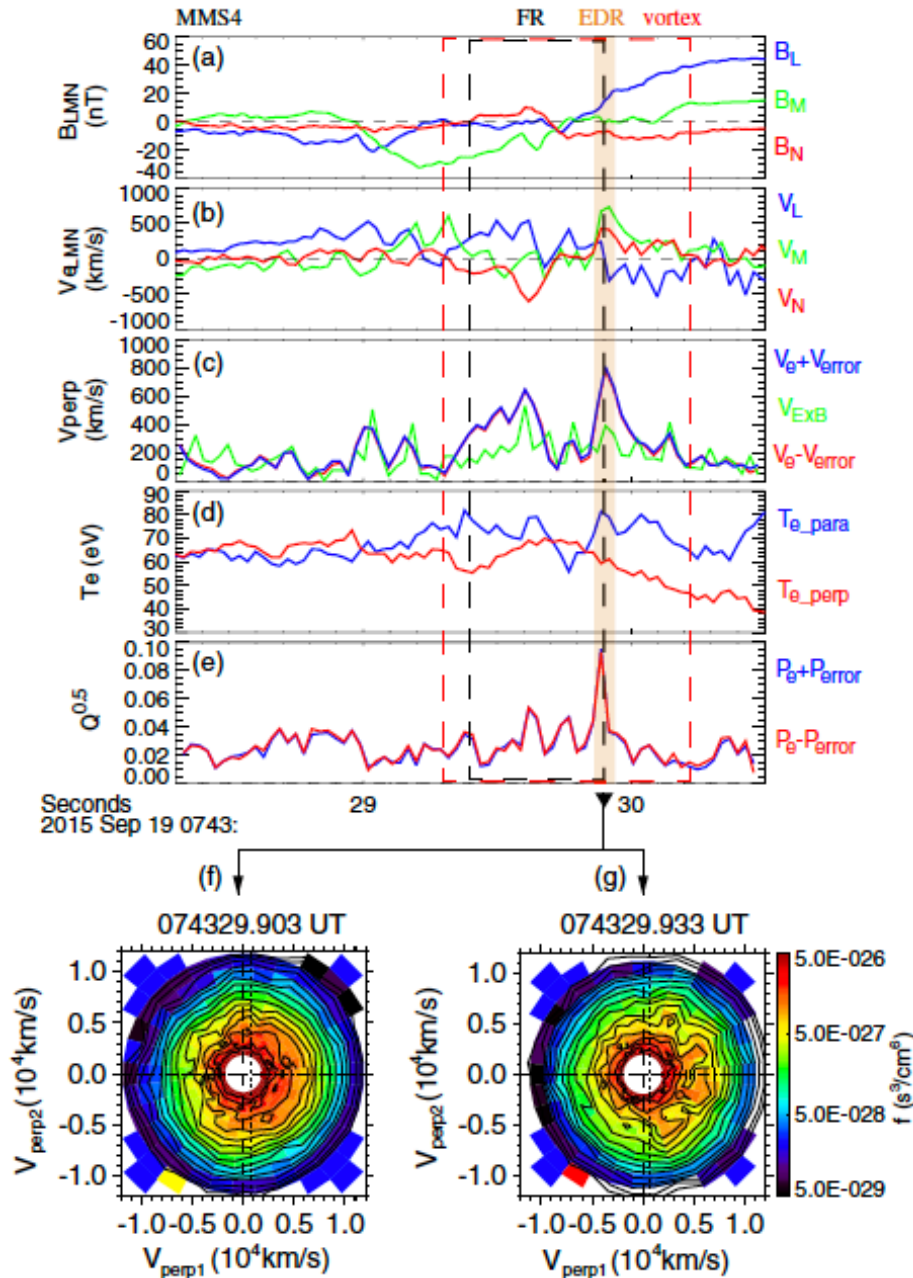
# Velocity-shear induced FTE



Dorelli & Bhattacharjee [2009]



# Velocity-shear induced FTE: electron-vortex induced FTE



Seconds 29.288 29.588 29.888 30.188 30.488  
2015 Sep 19 0743:

Zhong+ [2018]

# Velocity-shear induced FTE: 3-D PIC simulation

$L_x \times L_y \times L_z$

=  $100d_i \times 50d_i \times 150d_i$

=  $2048 \times 1024 \times 3072$  grids  $Z$

→  $1.2 \times 10^{12}$  total particles

$X$ : k-vector of KHI

$Y$ : boundary normal

$Z$ :  $X \times Y$

Mixing surfaces:

$F_e = -0.99, 0.99$

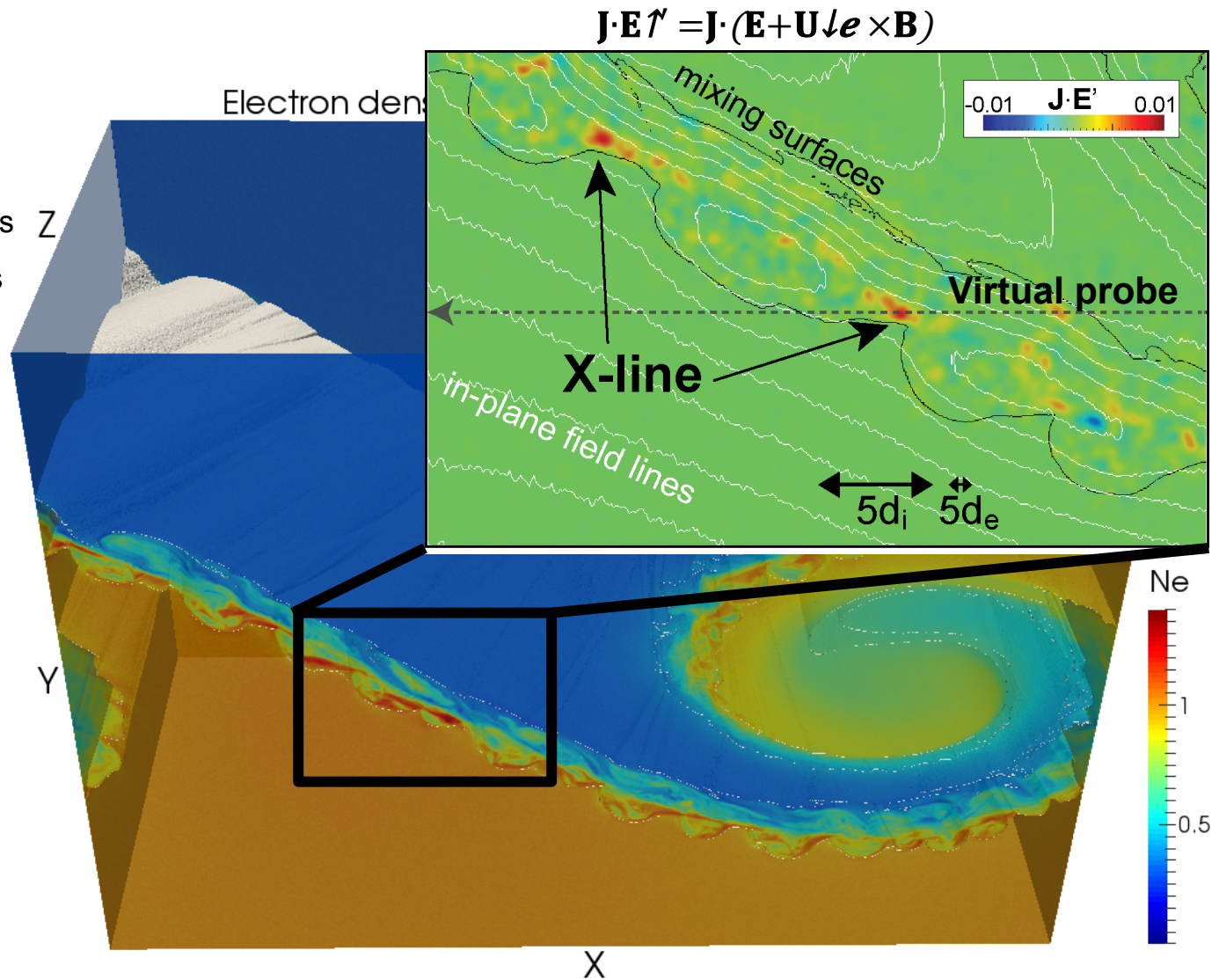
Mixing fraction:

$$F \equiv \frac{N_1 - N_2}{N_1 + N_2}$$

$F=1$ : Magnetosheath

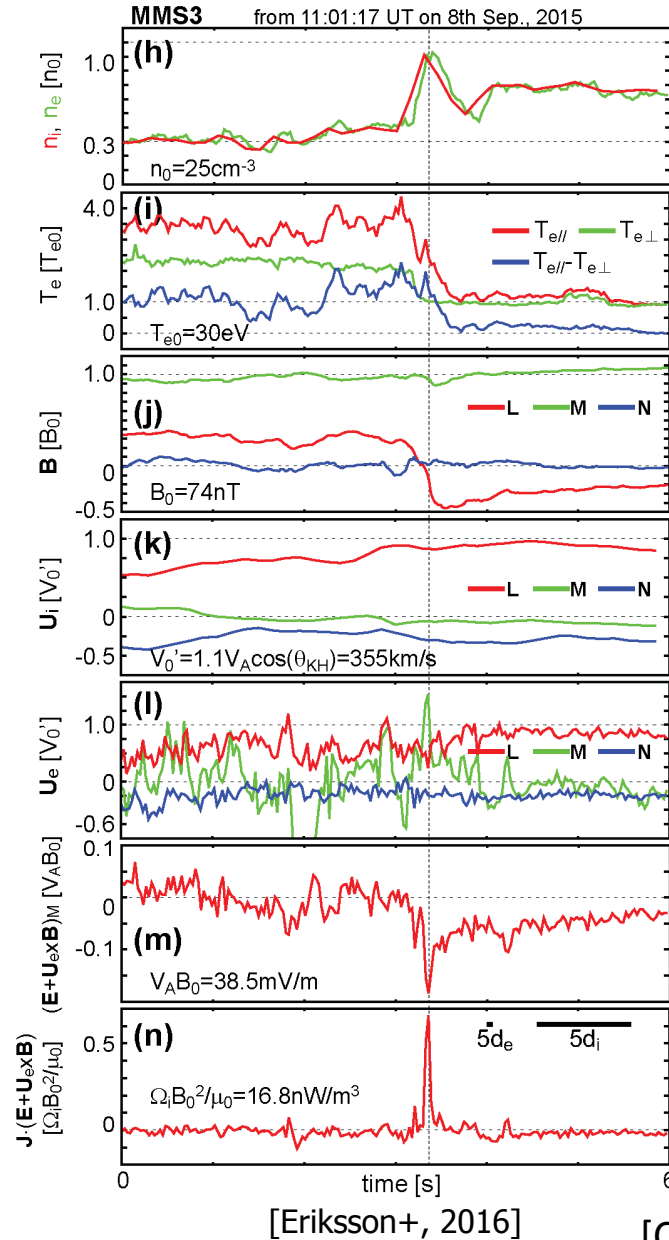
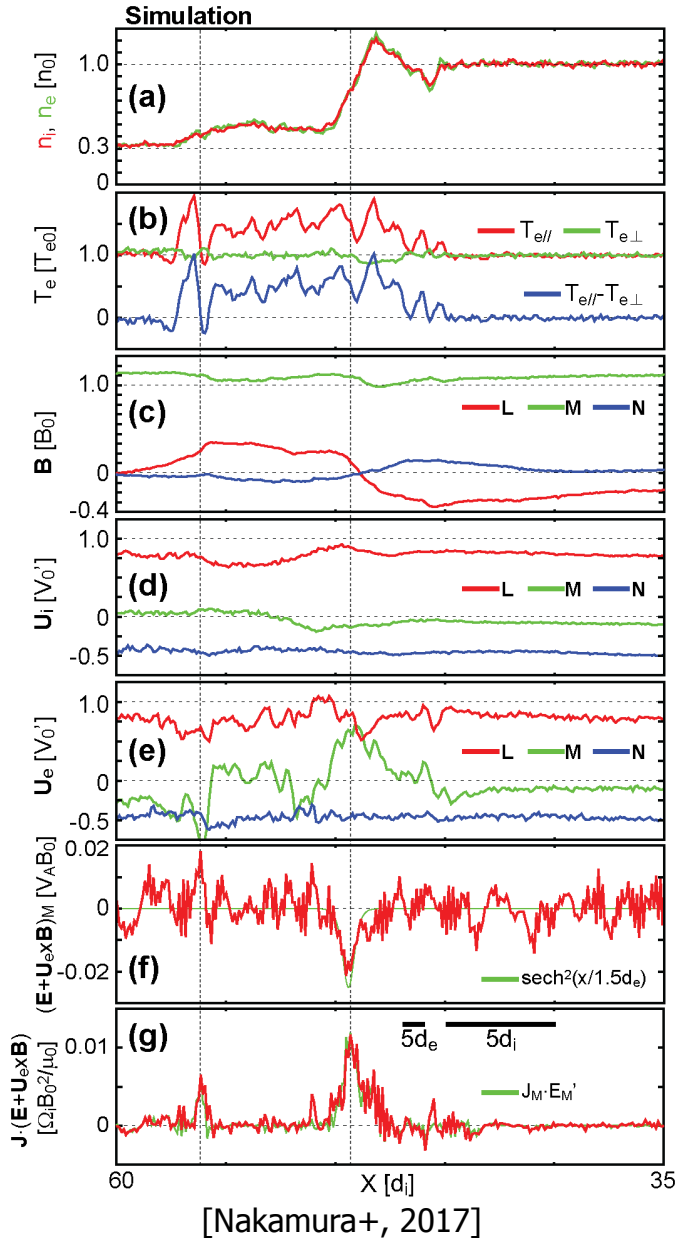
$F=-1$ : Magnetosphere

$|F| < 1$ : Mixing



[Nakamura+, 2017; Courtesy to T.K.M Nakamura]

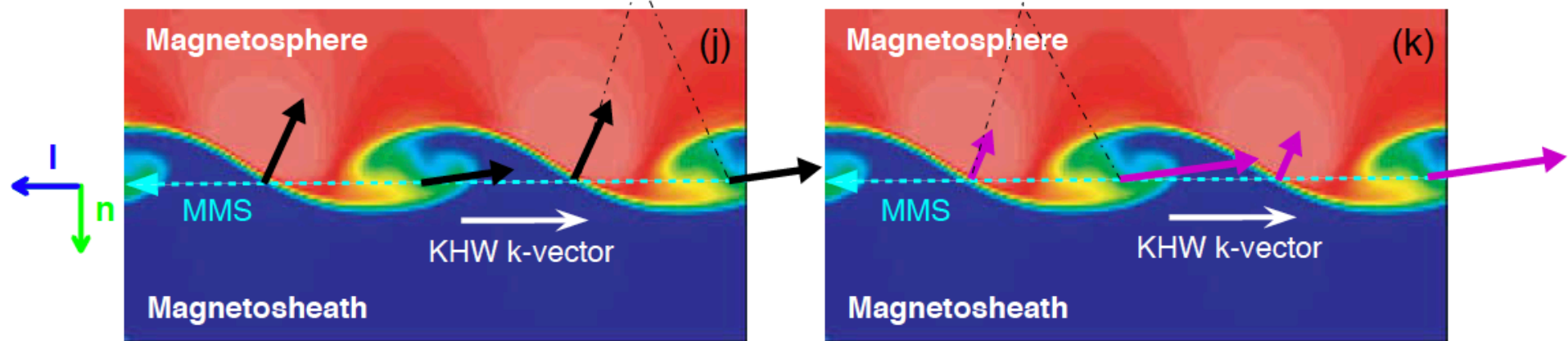
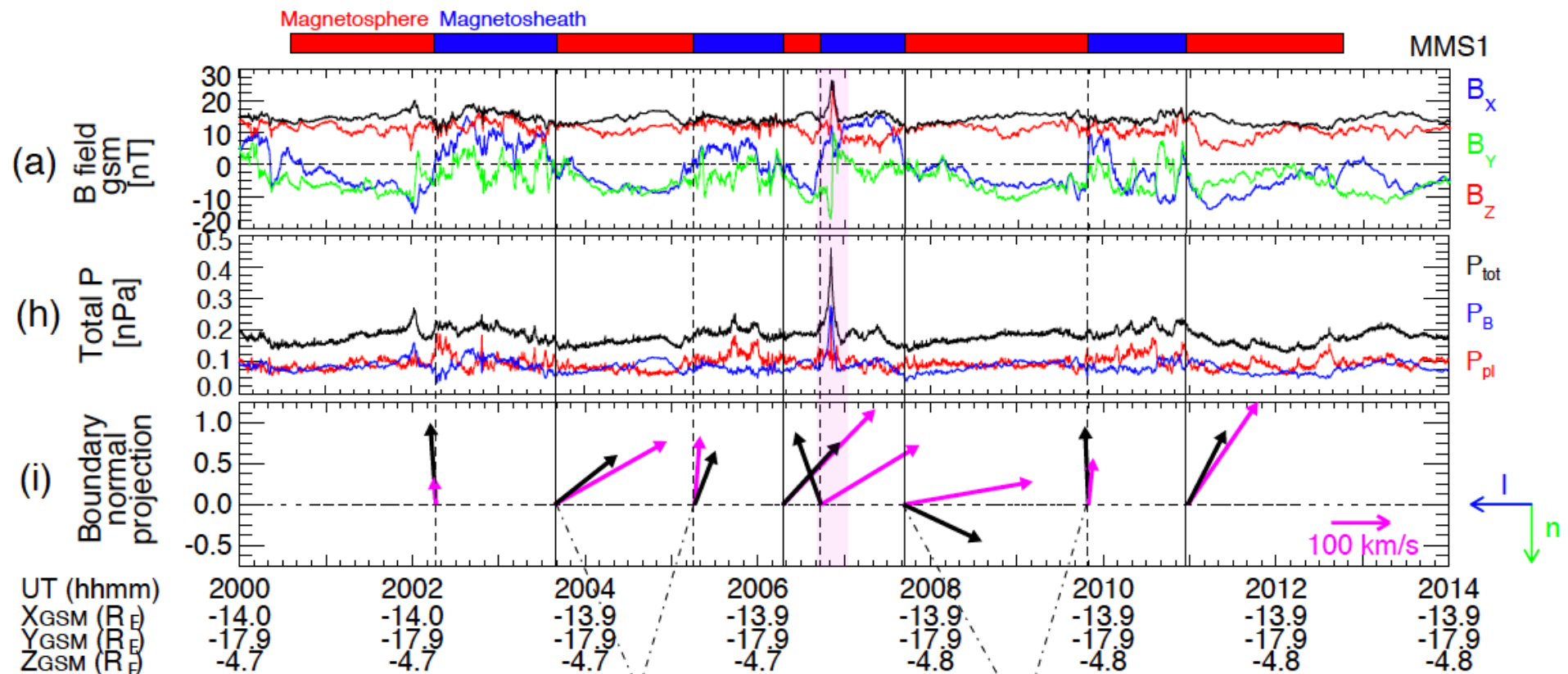
# Velocity-shear induced FTE: Comparison with Obs.



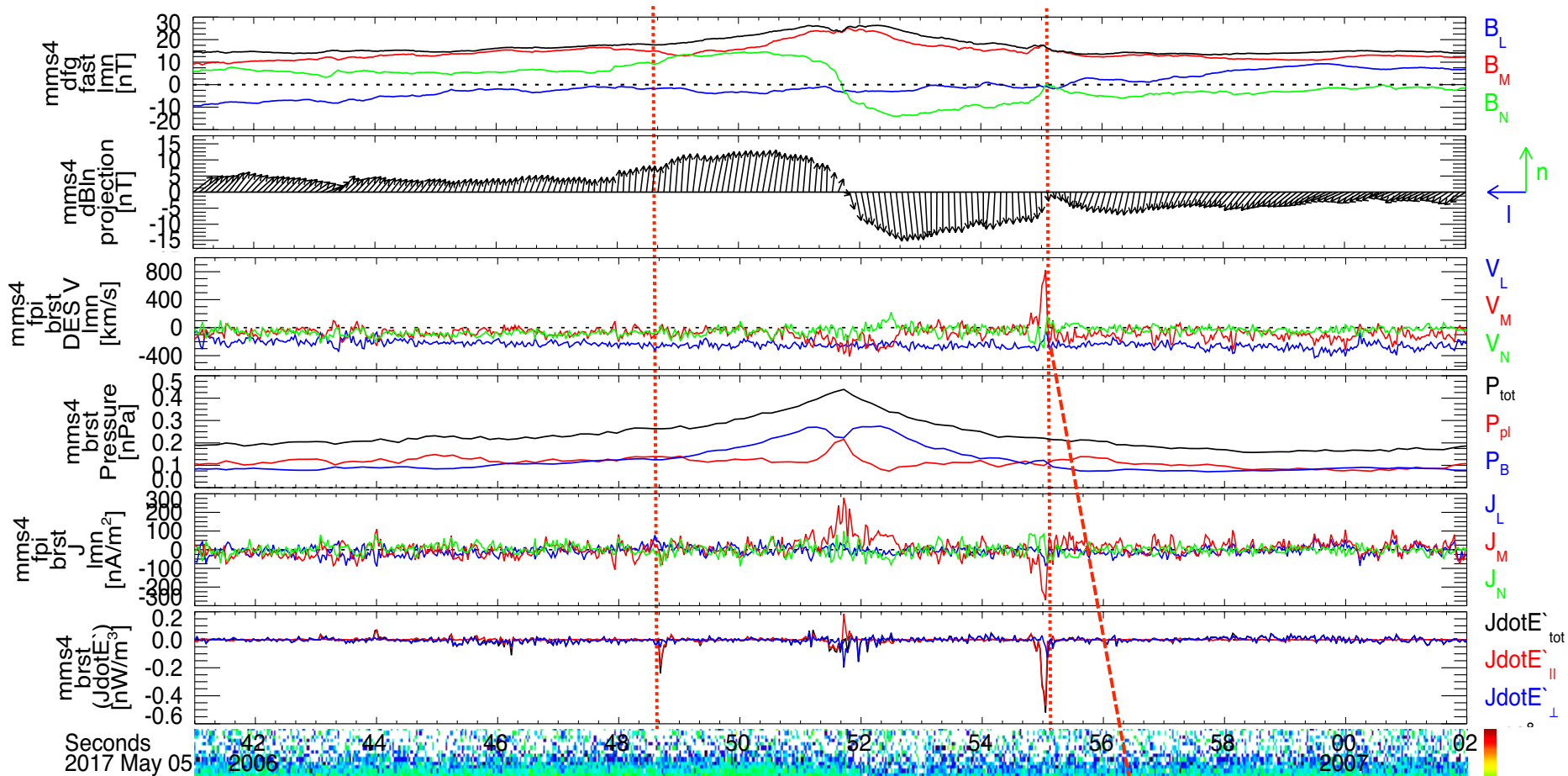
- Para electron heating
- Thin current sheet
- No ion jet
- No ele. Jet
- Current sustained by electron flow
- Strong  $E_M'$  (more than 5 times larger than 0.1 rate)
- $d_e$ -scale strong

[Courtesy to T.K.M Nakamura]

# KHV+FTE: FTE detected at the KHV boundary



# KHV+FTE: FTE detected at the KHV boundary

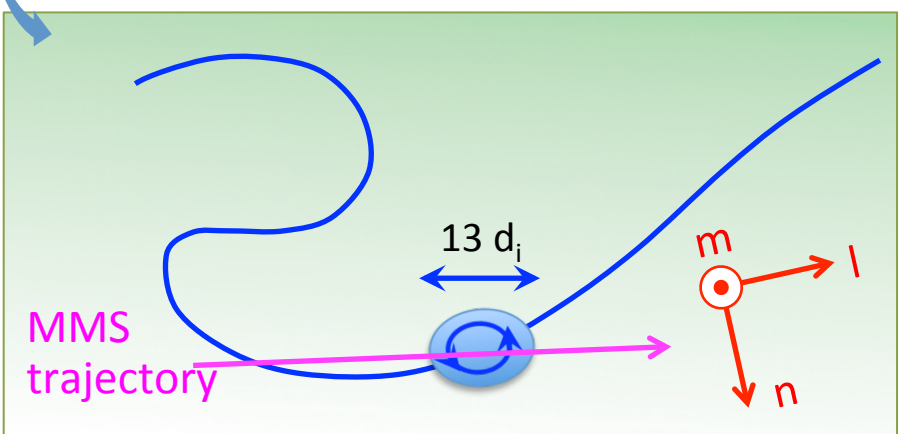
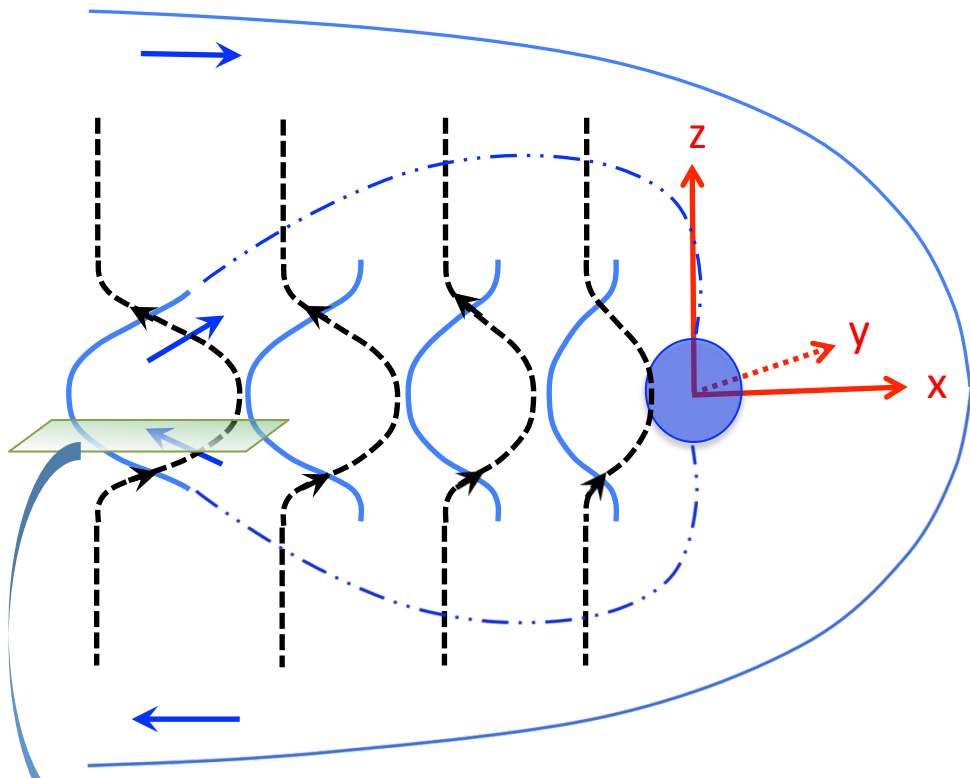


Similar to Nakamura+ [2017] and Eriksson+ [2016]...

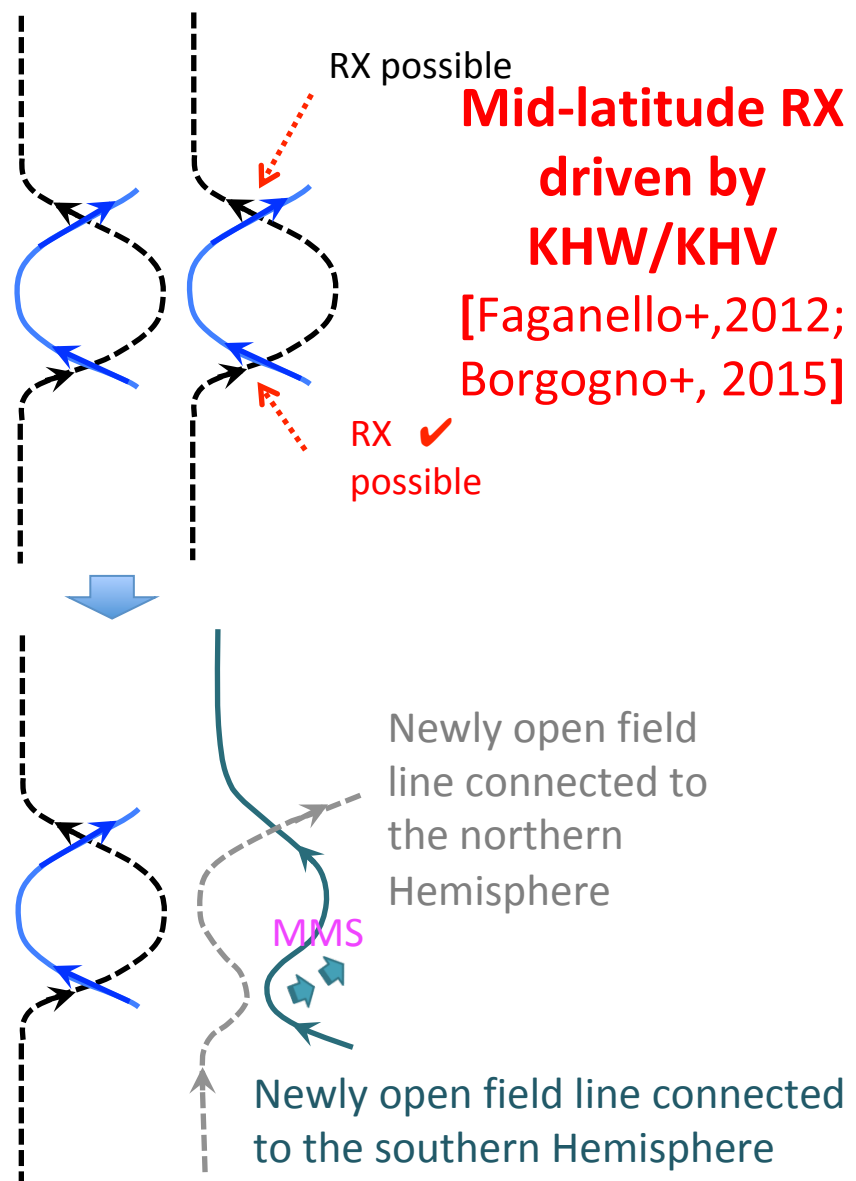
- Parallel electron heating
- no ion/electron in-plane jets
- Current carried by electrons
- Non-zero  $J \cdot E'$

“Strong northward electron jets”

# KHV+FTE: FTE detected at the KHV boundary



$5.4 R_E$



# Summary

## FTE

### Knowns

- General structure, motion, and extent
- IMF dependence
- Different models leading to different topology
- Substructure (partly)

### Unknowns

- Substructure (further details, variations)
- Energy conversion (partly answered by MMS)
- What regulates the contraction or expansion of FTEs? (related to force balance?)
- The relationship with ion/electron flow vortex

# Outline

1. **FTE: general knowns**
2. **Reconnection-based FTE models**
3. **New findings of FTE after MMS**
4. **Velocity-shear-induced FTE**

**Thank you!**